Available online at www.sciencedirect.com
ScienceDirect
Nuclear Physics A
Nuclear Physics A 00 (2018) 1–4
www.elsevier.com/locate/procedia
arXiv:1808.03238v2 [hep-ph]

XXVIIth International Conference on Ultrarelativistic Nucleus-Nucleus Collisions
(Quark Matter 2018)

Precision Dijet Acoplanarity Tomography of the Chromo Structure of Perfect QCD Fluids

M. Gyulassy[a,b,c,d], P. Levai[b], J. Liao[e,d], S. Shi[e], F. Yuan[a], X.N. Wang[a,d]

[a]*Nuclear Science Division, Lawrence Berkeley National Laboratory, Berkeley, CA 94720, USA*
[b]*MTA Wigner Research Centre for Physics, 1525 Budapest, Hungary*
[c]*Pupin Lab MS-5202, Department of Physics, Columbia University, New York, NY 10027, USA*
[d]*Institute of Particle Physics, Central China Normal University, Wuhan, China*
[e]*Physics Department and Center for Exploration of Energy and Matter, Indiana University, 2401 N Milo B. Sampson Lane, Bloomington, IN 47408, USA*

This is an update from my 2017 lecture at CCNU: see link
http://www.columbia.edu/~mg150/Talks/2017/MGyulassy-Lec2-CCNU-101817.pdf

Key references on which this work was built

A. H. Mueller, B. Wu, B. W. Xiao and F. Yuan,
Probing Transverse Momentum Broadening in Heavy Ion Collisions
Phys. Lett. B 763, 208 (2016)

Probing Transverse Momentum Broadening via Dihadron and Hadron-jet Angular Correlations in Relativistic Heavy-ion Collisions
Phys. Rev. D 95, 034007 (2017)

L. Chen, G. Y. Qin, S. Y. Wei, B. W. Xiao and H. Z. Zhang,
Probing Transverse Momentum Broadening via Dihadron and Hadron-jet Angular Correlations in Relativistic Heavy-ion Collisions
Phys. Lett. B 773, 672 (2017) [arXiv:1607.01932 [hep-ph]]

ALICE Collaboration: Measurement of jet quenching with semi-inclusive hadron-jet distributions in central Pb-Pb collisions at sNN = √2.76 TeV, JHEP1509 (2015)

STAR Collaboration: easurements of jet quenching with semi-inclusive hadron+jet distributions in Au+Au collisions at sNN=√ 200 GeV , Phys.Rev. C96 (2017)

Outline

Section 1: Introduction

Section 2: Some details of the calculation

Section 3: Numerical examples and conclusions

My interest in acoplanarity was motivated by a Peter Jacob question after my INT 2017 talk on

Consistency of Perfect Fluidity and Jet Quenching in semi-Quark-Gluon-Monopole-Plasmas (sQGMP)

Jiechen Xu , J.Liao, MG, Chin.Phys.Lett. 32 (2015) and JHEP 1602 (2016) 169
Shuzhe Shi, J.Xu, J.Liao, MG, Nucl.Phys. A967 (2017) 648
Shuzhe Shi, J.Liao, MG: Chin.Phys. C 42 (2018) 104104,

Global χ2 RHIC and LHC Data Constraints on Soft-Hard Transport Properties of sQGMP
[via CIBJET= EbE-VISHNU+CUJET3.1 , arXiv:1808.05461 [hep-ph]]

Peter Jacob's question (my paraphrase) :

Can **future** *high precision* dijet acoplanarity measurements help to falsify **sQGMP** or **wQGP** or **AdS-BH** models of the color structure of QCD perfect fluids?

Or is acoplanarity limited to the extraction of only one BDMS medium saturation scale, **Qs**, as is already determined by jet and dijet nuclear modification ratio data RAA(pT) and IAA ??

$$Q_s^2(a) \equiv \left\langle q_\perp^2 \frac{L}{\lambda} \right\rangle_a \equiv \int dt \sum_b \hat{q}_{ab}(x(t),t) \equiv \sum_b \int dt d^2 q_\perp \; q_\perp^2 \Gamma_{ab}(q_\perp, t)$$

Can acoplanarity ***distribution shapes*** help to extract information on the color d.o.f in near perfect QCD fluids and their microscopic differential scattering rates, Γ_{ab} , near T ~ T_c ?

$$\Gamma_{ab}(q_\perp, T) = \rho_b(T) d^2\sigma_{ab}(T)/d^2 q_\perp$$

Does any Γ_{ab} exhibit critical opalescence near Tc that could account for ~ perfect fluidity?

Jet Transport Coefficients = q_T^2 moment of $\sum_b \Gamma_{ab}(q_\perp, T)$ in CIBJET semiQGMP

$$\hat{q}_F(E,T) = \int_0^{6ET} dq_\perp^2 \frac{2\pi}{(\boldsymbol{q}_\perp^2 + f_E^2\mu^2(\boldsymbol{z}))(\boldsymbol{q}_\perp^2 + f_M^2\mu^2(\boldsymbol{z}))}\rho(T)$$

$$q(q+g) \quad \left\{ [C_{qq}f_q + C_{qg}f_g] \cdot \boxed{[\alpha_s^2(\boldsymbol{q}_\perp^2)]} \cdot [f_E^2\boldsymbol{q}_\perp^2 + f_E^2 f_M^2\mu^2(\boldsymbol{z})] + \right.$$

$$qm \quad \left. [C_{qm}(1 - f_q - f_g)] \cdot \boxed{[1]} \cdot [f_M^2\boldsymbol{q}_\perp^2 + f_E^2 f_M^2\mu^2(\boldsymbol{z})] \right\}, \quad (14)$$

$$\hat{q}_g(E,T) = \int_0^{6ET} dq_\perp^2 \frac{2\pi}{(\boldsymbol{q}_\perp^2 + f_E^2\mu^2(\boldsymbol{z}))(\boldsymbol{q}_\perp^2 + f_M^2\mu^2(\boldsymbol{z}))}\rho(T)$$

$$g(q+g) \quad \left\{ [C_{gq}f_q + C_{gg}f_g] \cdot \boxed{[\alpha_s^2(\boldsymbol{q}_\perp^2)]} \cdot [f_E^2\boldsymbol{q}_\perp^2 + f_E^2 f_M^2\mu^2(\boldsymbol{z})] + \right.$$

$$gm \quad \left. [C_{gm}(1 - f_q - f_g)] \cdot \boxed{[1]} \cdot [f_M^2\boldsymbol{q}_\perp^2 + f_E^2 f_M^2\mu^2(\boldsymbol{z})] \right\}, \quad (15)$$

Note Γ_{qm} **&** Γ_{gm} **=> Critical Opalescence near Tc because** $\alpha_E \alpha_M = 1 >> \alpha_E^2$ (Dirac)

Can acoplanarity *distribution shapes test the existence of such novel color dynamics in* ≈ Perfect QCD fluids near Tc and constrain the multicomponent differential scattering rates?

$$\Gamma_{ab}(q_\perp, T) = \rho_b(T) d^2\sigma_{ab}(T)/d^2 q_\perp$$

Note that CUJET dE/dL is ***not*** proportional to qhat L but given by a generalized DGLV formula

(See eq2.23 J.Xu, J.Liao, MG, JHEP 02 (2016) 169)

Dijet acoplanarity is an A+B observable among many needed to help falsify models of A+A dynamics and probe deeper into the unknown the color structure of QCD perfect fluids produced at RHIC and LHC

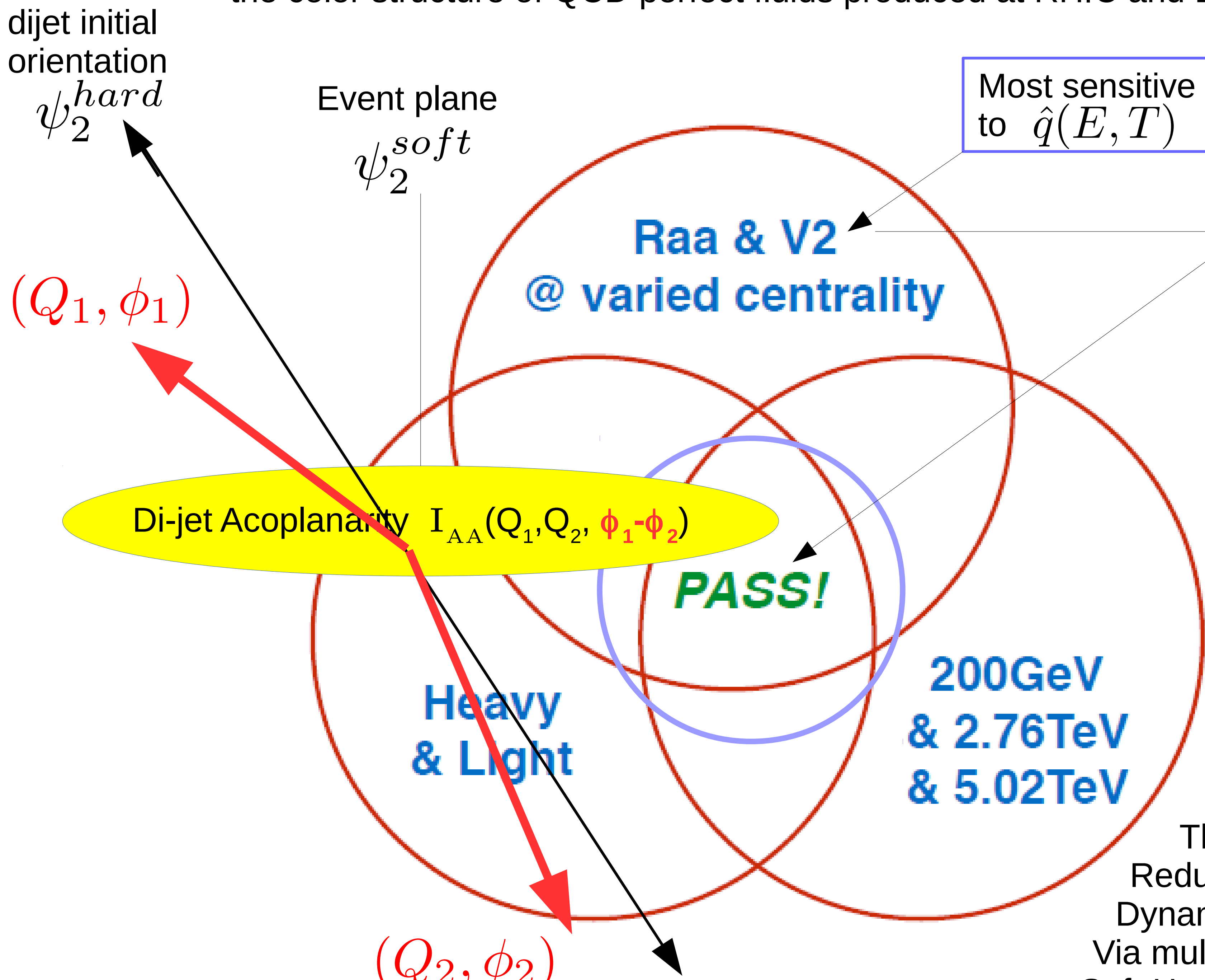

The challenge is to Reduce the Volume of Dynamical A+A models Via multiple independent Soft-Hard exp constraints

Monopole component near Tc
could account for near perfect fluidity

$$\frac{d\sigma_{EM}}{dq_\perp^2} \sim \frac{\alpha_E\alpha_M}{q_\perp^4} \sim \frac{1}{\alpha_E^2}\frac{d\sigma_{EE}}{dq_\perp^2} \gg \frac{d\sigma_{EE}}{dq_\perp^2}$$

Ed Shuryak
Jinfeng Liao

From "Transparency" to Opaqueness

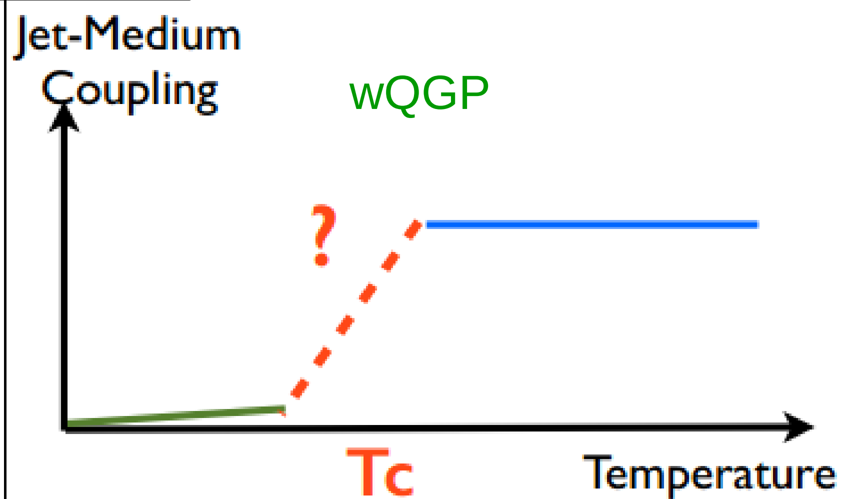

"Waterfall" scenario

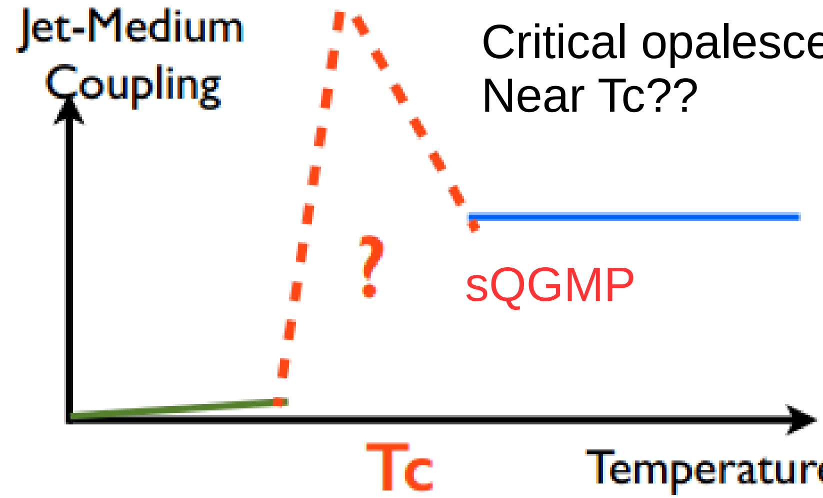

"Volcano" scenario

The temperature dependence of jet-medium coupling has profound consequences!

J.Liao 2015

CIBJET was developed by A. Buzzatti, J.Xu, Shuzhe Shi, Jinfeng Liao, MG to test quantitatively this idea with SPS, RHIC and LHC RAA, v2, v3 data

Quantitative Test of “Volcano scenario”with CIBJET sQGMP

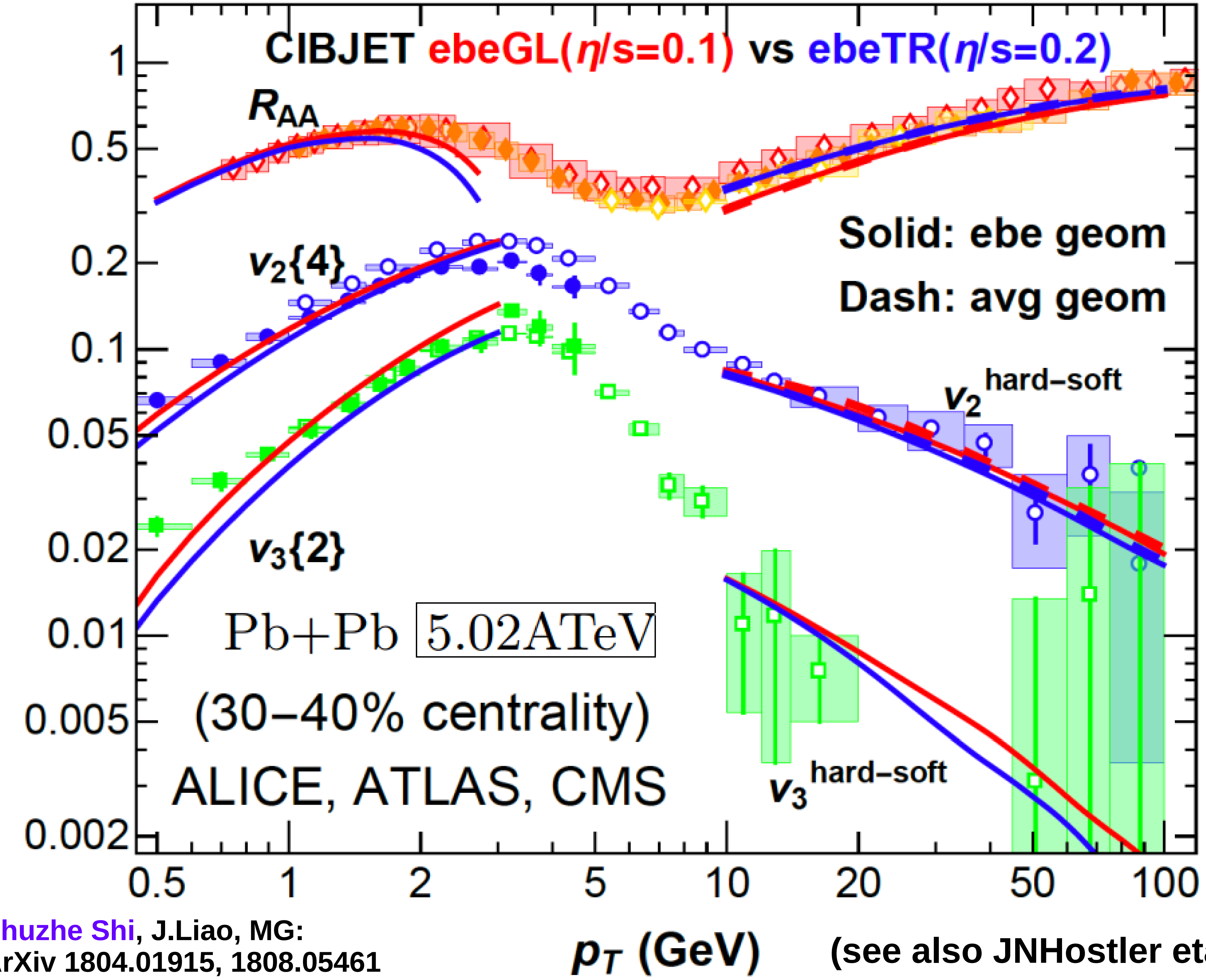

Shuzhe Shi, J.Liao, MG:
ArXiv 1804.01915, 1808.05461

(see also JNHostler etal 2016)

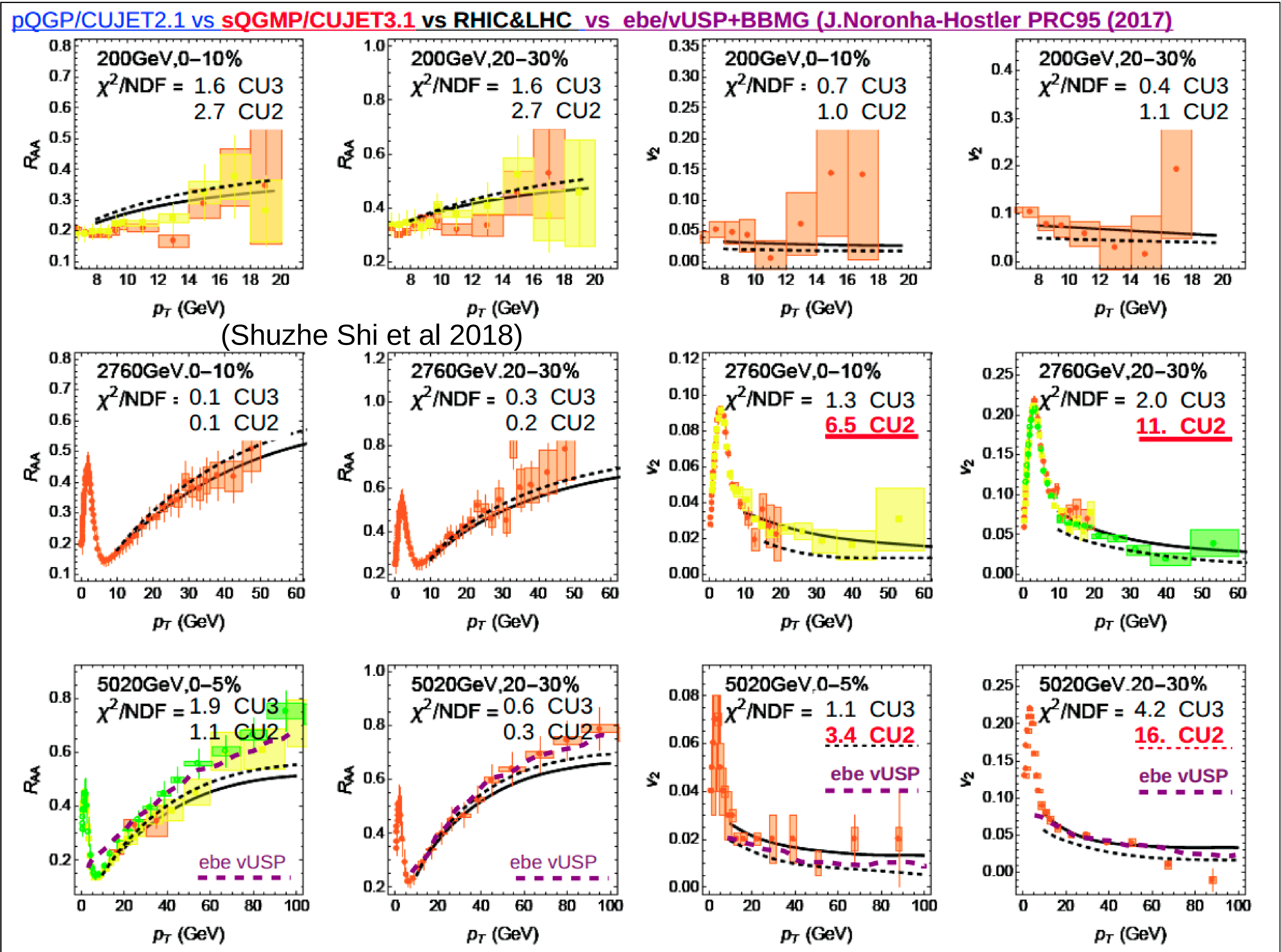
pQGP/CUJET2.1 vs sQGMP/CUJET3.1 vs RHIC&LHC vs ebe/vUSP+BBMG (J.Noronha-Hostler PRC95 (2017)
200GeV,0–10%
χ²/NDF = 1.6 CU3
2.7 CU2
200GeV,20–30%
χ²/NDF = 1.6 CU3
2.7 CU2
200GeV,0–10%
χ²/NDF : 0.7 CU3
1.0 CU2
200GeV,20–30%
χ²/NDF = 0.4 CU3
1.1 CU2
(Shuzhe Shi et al 2018)
2760GeV.0–10%
χ²/NDF : 0.1 CU3
0.1 CU2
2760GeV.20–30%
χ²/NDF = 0.3 CU3
0.2 CU2
2760GeV,0–10%
χ²/NDF = 1.3 CU3
6.5 CU2
2760GeV,20–30%
χ²/NDF = 2.0 CU3
11. CU2
5020GeV,0–5%
χ²/NDF = 1.9 CU3
1.1 CU2
ebe vUSP
5020GeV,20–30%
χ²/NDF = 0.6 CU3
0.3 CU2
ebe vUSP
5020GeV,0–5%
χ²/NDF = 1.1 CU3
3.4 CU2
ebe vUSP
5020GeV,20–30%
χ²/NDF = 4.2 CU3
16. CU2
ebe vUSP
R_AA
v_2
p_T (GeV)

Shuzhe Shi etal arXiv:1808.05461 [hep-ph],

VISHNU ⊗ **CUJET3.1**

Global RHIC+LHC1+LHC2 RAA+v2 $\chi^2(\alpha_c, c_m)$ fit contours

sQGMP=(Suppressed $\chi_T^L = c_q L + c_g L^2$ elec semi-Q+G) + (Emergent $(1-\chi_T^L)$ mag.monopoles)

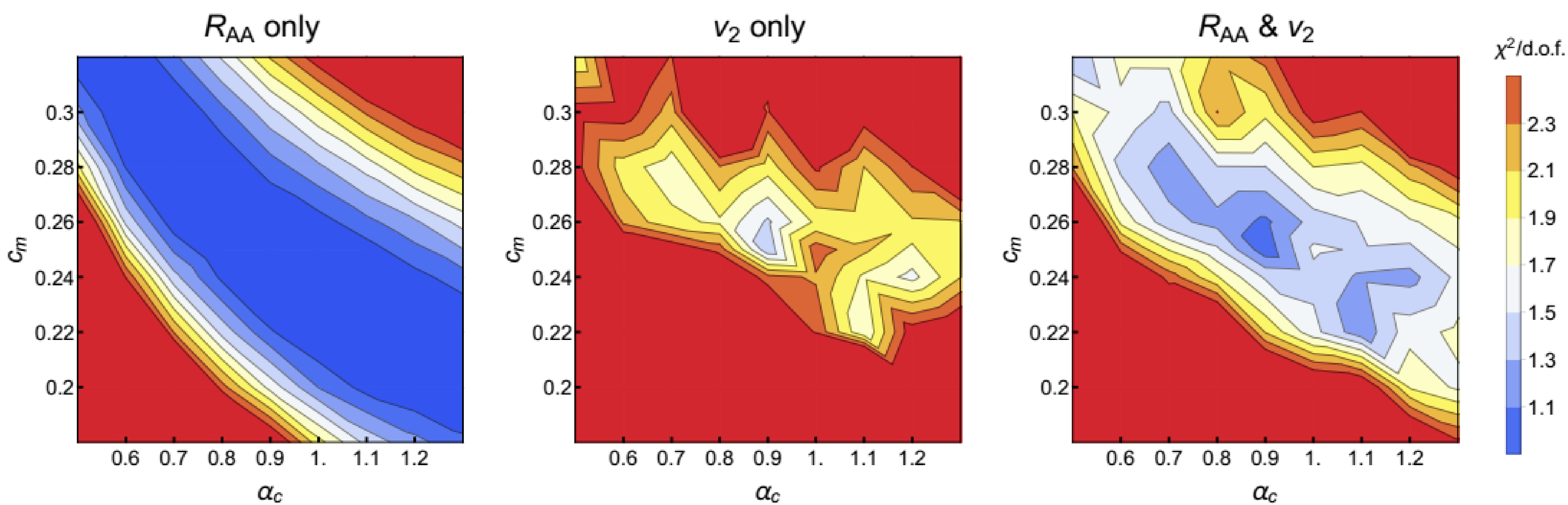

FIG. 1: (color online) χ^2/d.o.f. comparing χ_T^L-scheme CUJET3 results with RHIC and LHC data. Left: χ^2/d.o.f. for R_{AA} only. Middle: χ^2/d.o.f. for v_2 only. Right: χ^2/d.o.f. including both R_{AA} and v_2

With CIBJET = ***ebe*** IC+VISHNU+CUJET3.1 framework

Shuzhe Shi found that ebe only makes ~10% changes to hard v2 relative using event ave geom.

There is tension between CIBJET and vUSPhydro SHEE framework interpretations, but CIBJET qhat has the advantage that it bridges jet quenching with perfect fluidity

Shuzhe Shi, J.Liao, MG: arXiv:1804.01915 and **1808.05461**

Quantitative extraction of $\hat{q}_F(E,T)$ jet transport field and $\eta/s(T)$ via CIBJET

The q+g suppressed semi-QGP components of **sQGMP** require large monopole density near Tc to compensate the loss of color electric dof and still fit the lattice Eq of State: P/T or S(T)

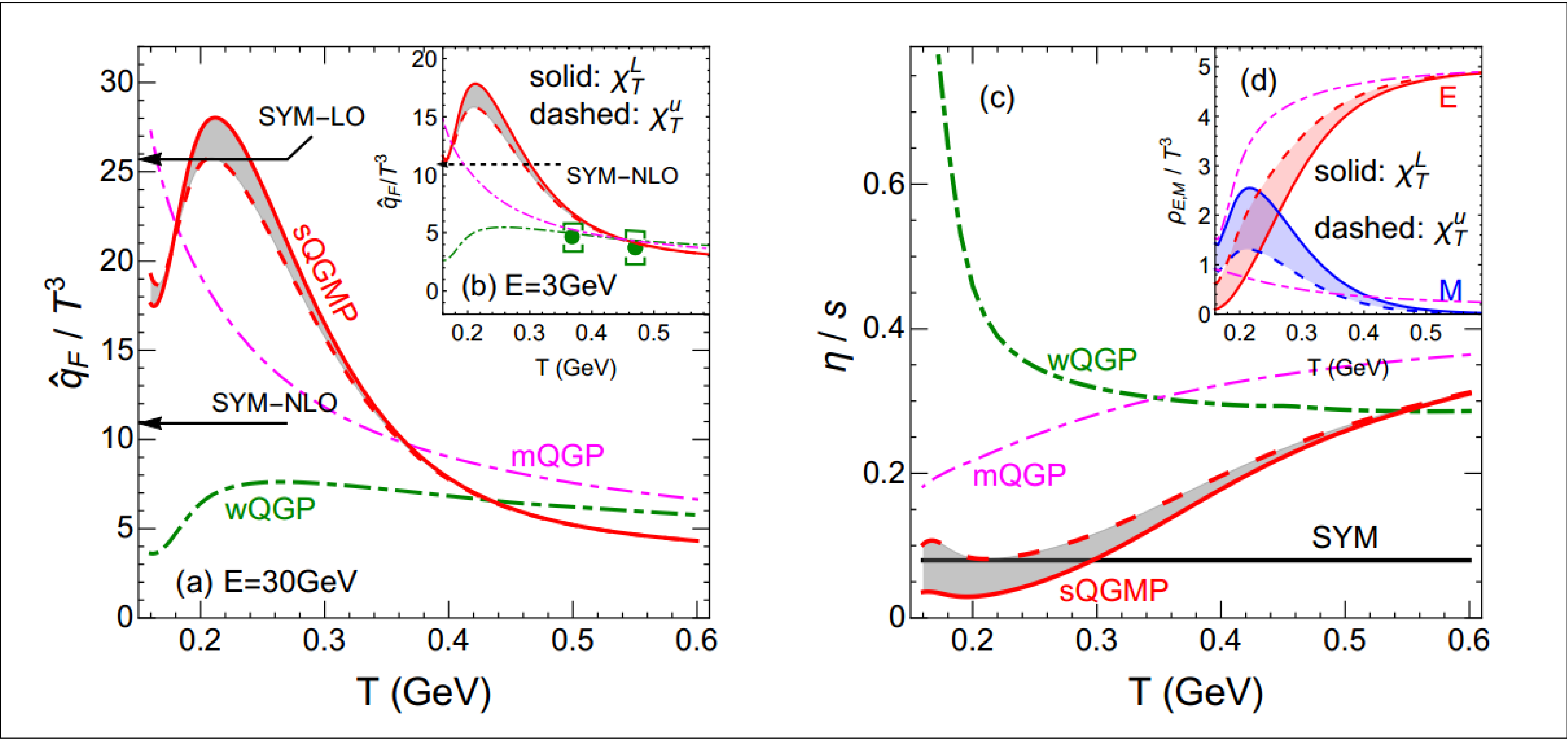

Lattice constrained sQGMP color composition model accounts not only for global RHIC&LHC RAA, v2, v3 data but uniquely accounts for bulk perfect fluidity due to Near unitary bound q+m and g+m scattering rate near Tc !

Can we learn ***more*** about the QCD perfect fluid color structure than just its average BDMS second moment jet transport parameter? $Q_{sat}^2 = \langle \hat{q} L \rangle = \langle \chi \mu^2 \rangle$

Can we determine the **opacity** $\chi = L/\lambda(T)$ and the **screening scale** $\mu(T)$ ***separately*** Using future precise data on the Landau and Rutherford multiple scattering **tails** of the acoplanarity distribution ?

Sudakov ⊗ BDMS Gaussian “**Ears**”

$$\exp[-\delta\phi^2/(Q_s/Q)^2]$$

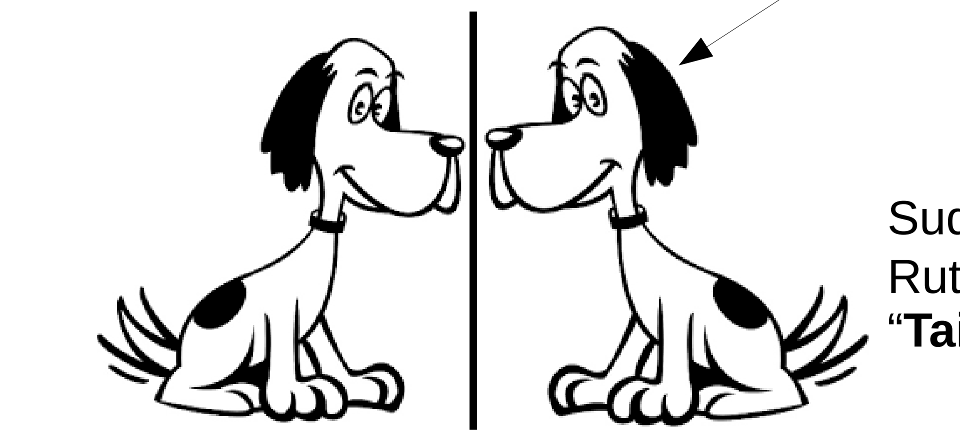

$-3\pi/4$ π $+3\pi/4$

$$\Delta\phi = \phi_1 - \phi_2 = \pi - \delta\phi$$

Sudakov ⊗
Rutherford
“**Tails**”

$$\sim \frac{\alpha}{\delta\phi^2} + \frac{(Q_s/Q)^2}{\delta\phi^4}$$

$\vec{Q}_1 = \vec{Q} + \vec{q}/2$

$\vec{q}$

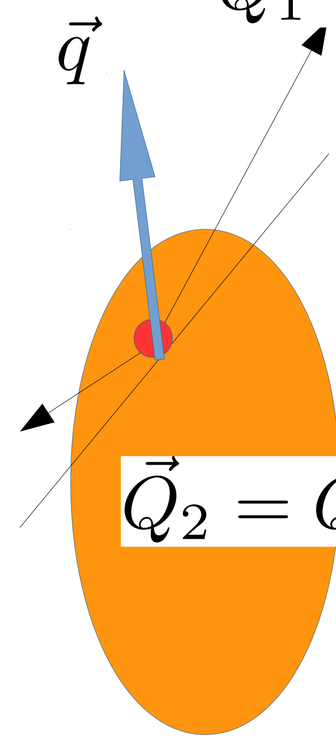

$\vec{Q}_2 = \vec{Q} - \vec{q}/2$

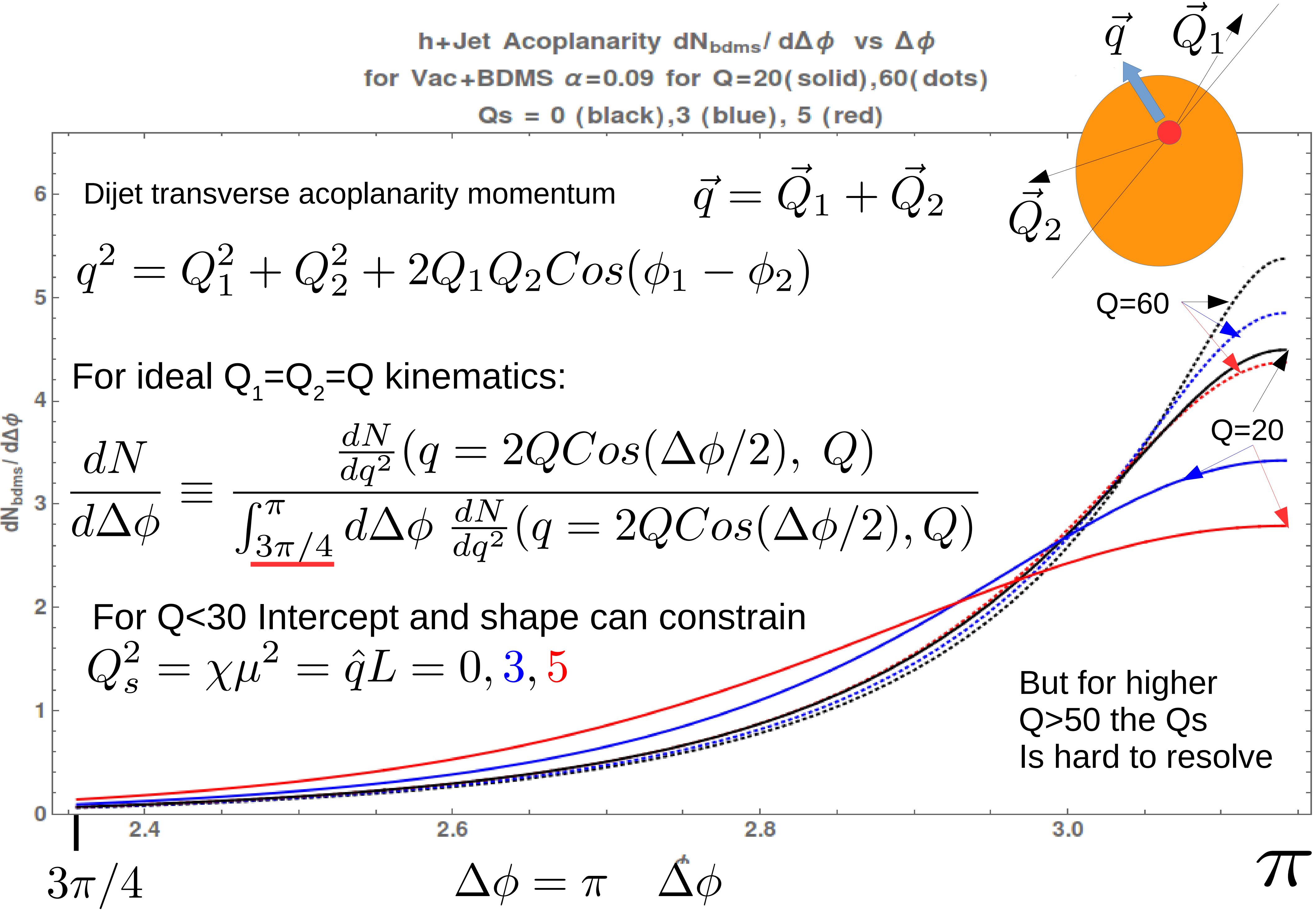
h+Jet Acoplanarity $dN_{bdms}/d\Delta\phi$ vs $\Delta\phi$
for Vac+BDMS α=0.09 for Q=20(solid),60(dots)
Qs = 0 (black),3 (blue), 5 (red)
Dijet transverse acoplanarity momentum
$\vec{q} = \vec{Q}_1 + \vec{Q}_2$
$\vec{q}$
$\vec{Q}_1$
$\vec{Q}_2$
$q^2 = Q_1^2 + Q_2^2 + 2Q_1Q_2Cos(\phi_1 - \phi_2)$
For ideal Q_1=Q_2=Q kinematics:
$\frac{dN}{d\Delta\phi} \equiv \frac{\frac{dN}{dq^2}(q = 2QCos(\Delta\phi/2),\ Q)}{\int_{3\pi/4}^{\pi} d\Delta\phi\ \frac{dN}{dq^2}(q = 2QCos(\Delta\phi/2), Q)}$
For Q<30 Intercept and shape can constrain
$Q_s^2 = \chi\mu^2 = \hat{q}L = 0, 3, 5$
Q=60
Q=20
But for higher
Q>50 the Qs
Is hard to resolve
$dN_{bdms}/d\Delta\phi$
0
1
2
3
4
5
6
2.4
2.6
2.8
3.0
$3\pi/4$
$\Delta\phi = \pi \quad \hat{\Delta\phi}$
π

Lin Chen, Guang-You Qin *, Shu-Yi Wei, Bo-Wen Xiao, Han-Zhong Zhang PLB 773 (2017) 672
"Probing transverse momentum broadening in gamma-jet

distribution in the Sudakov resummation formalism as follows

$$\frac{d\sigma}{d\Delta\phi} = \sum_{a,b,c,d} \int p_{\perp\gamma} dp_{\perp\gamma} \int p_{\perp J} dp_{\perp J} \int dy_\gamma \int dy_J \int db \times x_a f_a(x_a, \mu_b) x_b f_b(x_b, \mu_b) \frac{1}{\pi} \frac{d\sigma_{ab\to cd}}{d\hat{t}} b\, J_0(|\vec{q}_\perp|b) \boxed{e^{-S(Q,b)},} \tag{1}$$

where J_0 is the Bessel function of the first kind, $q_\perp$ is the transverse momentum imbalance between the photon and the jet $\vec{q}_\perp \equiv \vec{p}_{\perp\gamma} + \vec{p}_{\perp J}$, which takes into account both initial and final transverse momentum kicks from vacuum Sudakov radiations and medium gluon radiations. Here we define $x_{a,b} = max(p_{\perp\gamma}, p_{\perp J})(e^{\pm y_\gamma} + e^{\pm y_J})/\sqrt{s_{NN}}$ as

The vacuum Sudakov factor $S_{pp}(Q, b)$ is defined as

$$S_{pp}(Q, b) = S_P(Q, b) + S_{NP}(Q, b) \tag{2}$$

where the perturbative S_P Sudakov factor depends on the incoming parton flavour and outgoing jet cone size. The perturbative Sudakov factors can be written as [35–37]

pQCD Vacuum Shower

$$S_P(Q, b) = \sum_{q,g} \int_{\mu_b^2}^{Q^2} \frac{d\mu^2}{\mu^2} \left[A \ln \frac{Q^2}{\mu^2} + B + D \ln \frac{1}{R^2} \right] \tag{3}$$

At the next-to-leading-log (NLL) accuracy, the coefficients can be expressed as $A = A_1 \frac{\alpha_s}{2\pi} + A_2 (\frac{\alpha_s}{2\pi})^2$, $B = B_1 \frac{\alpha_s}{2\pi}$ and $D = D_1 \frac{\alpha_s}{2\pi}$, with the value of individual terms given by the following table, where both A and B terms are summed over the corresponding incoming parton flavours.

	A_1	A_2	B_1	D_1
quark	C_F	$K \cdot C_F$	$-\frac{3}{2} C_F$	C_F
gluon	C_A	$K \cdot C_A$	$-2\beta C_A$	C_A

Here C_A and C_F are the gluon and quark Casimir factor, respectively. $\beta = \frac{11}{12} - \frac{N_f}{18}$, and $K = (\frac{67}{18} - \frac{\pi^2}{6}) C_A - \frac{10}{9} N_f T_R$. $R^2 = \Delta\eta^2 + \Delta\phi^2$ represents the jet cone-size, which is set to match the experimental setup. The implementation of the non-perturbative Sudakov factor $S_{NP}(Q, b)$ follows the prescription given in Refs [61, 62]. In the Sudakov resummation formalism, following the usual b^* prescription, the factorization scale is set to be $\mu_b \equiv \frac{c_0}{b_\perp} \sqrt{1 + b_\perp^2 / b_{max}^2}$,

Jet-hadron acoplanarity azimuthal distribution from Chen,Qin,Xiao,Zhang PLB773, 2017
A+A Vacuum Sudakov+ BDMS(Qs) model compared to RHIC and LHC data

Current Status of A+A dijet acoplanarity at RHIC and LHC

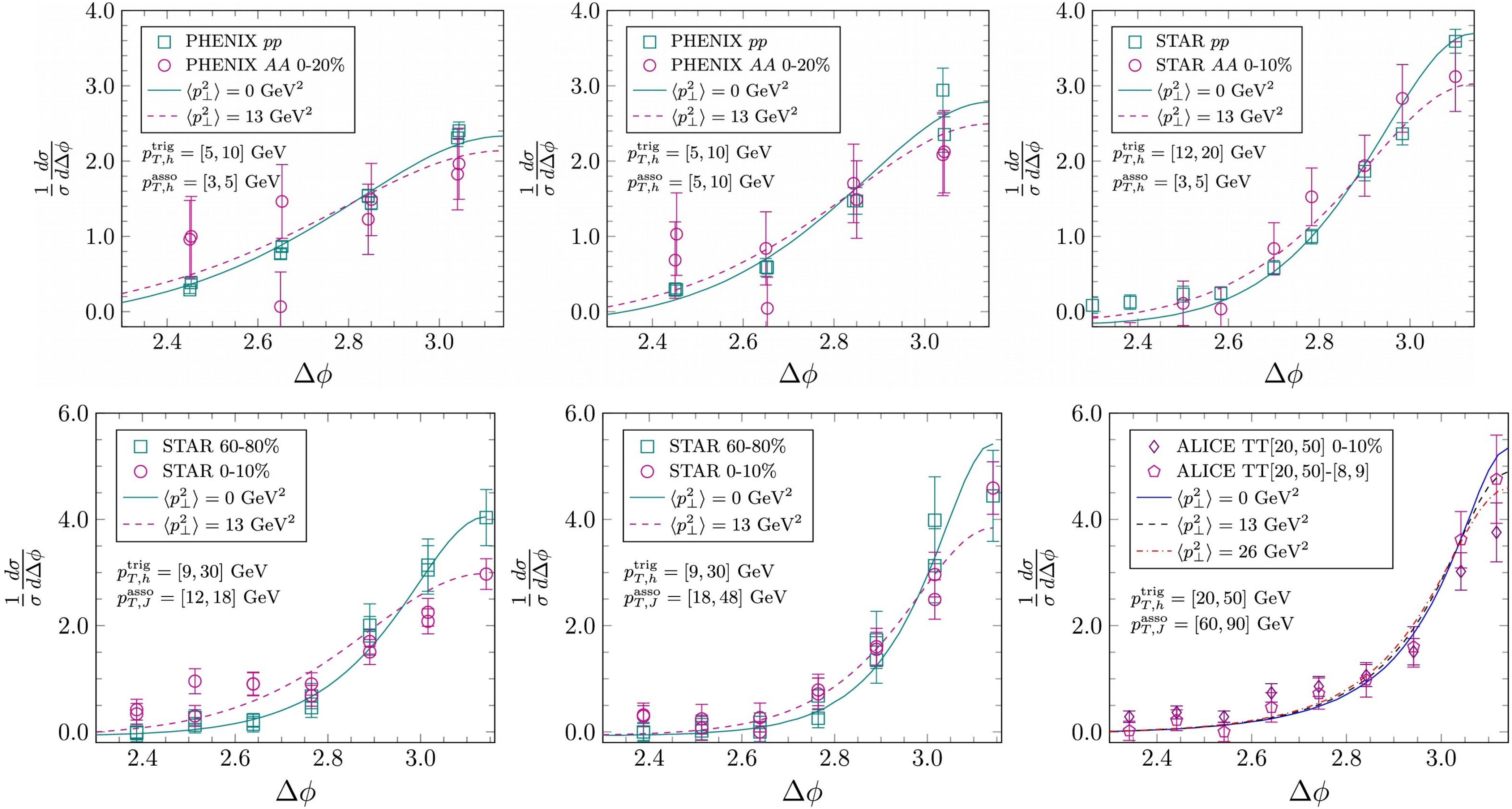

[Current exp precision does not constrain Qs or qhat better than RAA(pT) & v2(pT) already do.
Much higher precision future data needed in order to test color dof $n_a(T)$ and $d\sigma_{ab}/dq^2$ with acopl

CMS Studies of dijet transverse momentum imbalance and acoplanarity distributions in pPb collisions at 5.02 TeV have achieved great precision

2951 Page 6 of 26 Eur. Phys. J. C (2014) 74:2951

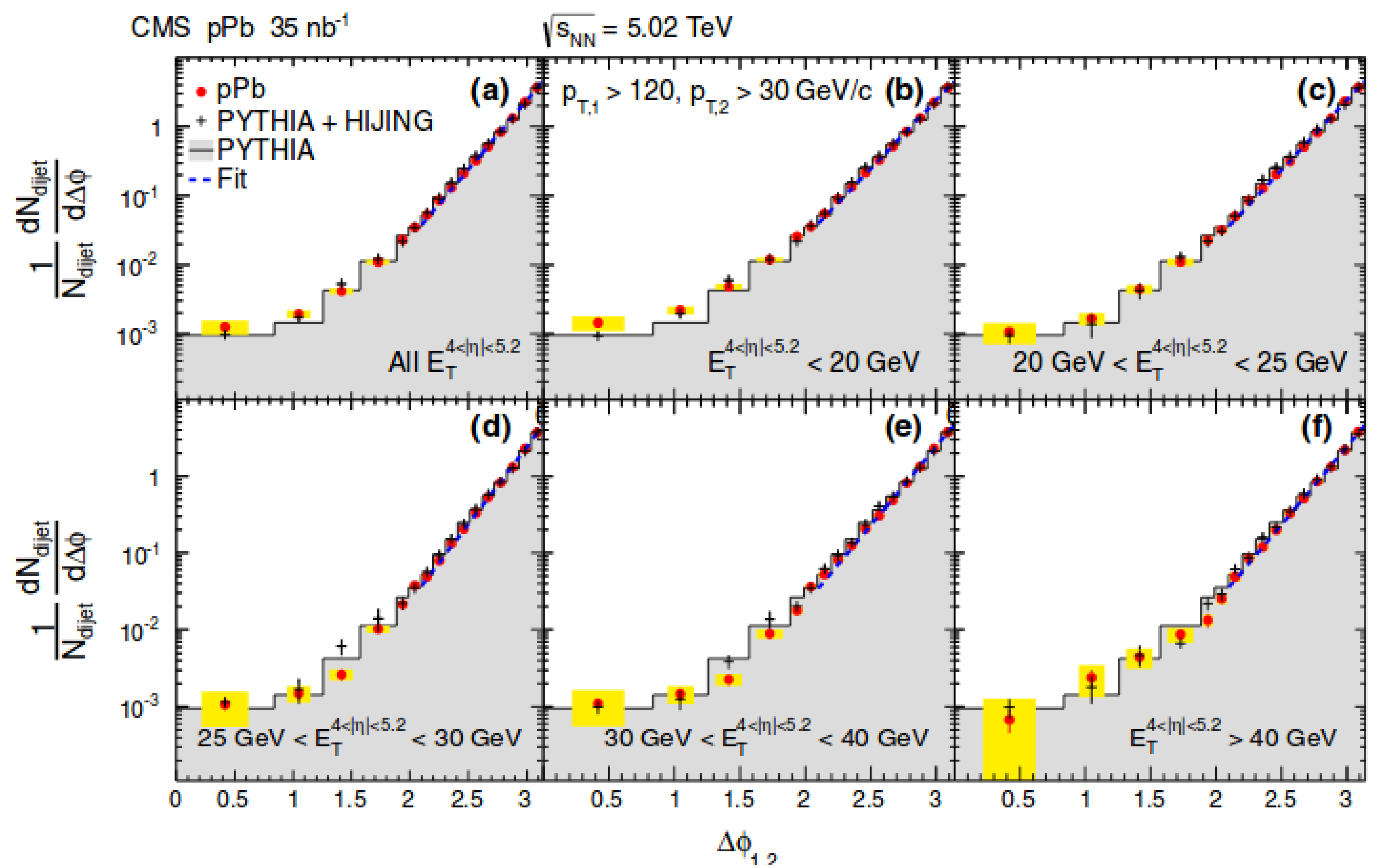

Very high precision has (after 30 years) been reached at LHC in pp and pA to quantify ***vacuum*** induced Sudakov acoplanarity due to jet gluon showers. Thus pQCD Sudakov (A, B and D) factors can now be tuned to higher accuracy. Small deviations from Sudakov distribution due to jet-medium multiple collision interactions can thus help to discriminate between competing models of the color structure of QCD perfects fluids in A+A reactions

Multiple jets and γ-jet correlation in high-energy heavy-ion collisions

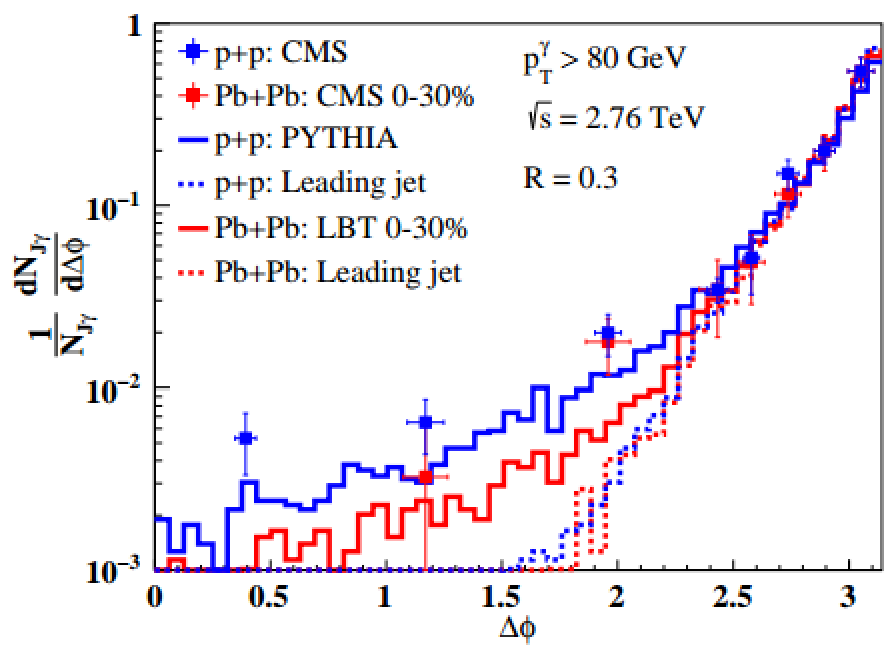

FIG. 6: (Color online) Angular distribution of γ-jet in central (0–30%) Pb+Pb (red) and p+p collisions (blue) at $\sqrt{s} = 2.76$

Luo,Cao,He,Wang CCNU
PLB782 (2018) , 1803.06785 [

High pT~ 100 GeV makes small angle Deviations from pi nearly independent Of medium effect and are dominated by Vacuum Sudakov radiation effects.

At large angles < 2 there is a predicted suppression of gamma-jet correlations due to multiple induced medium response

Exp should focus on the “sweet window”

$$2.4 < \Delta\phi < \pi$$

To reduce distortion due to quenching of gluon showers and medium recoil contributions

“Dominance of the Sudakov form factor in γ-jet correlation from soft gluon radiation in large pT hard processes pose a challenge for using γ-jet azimuthal correlation to study medium properties via large angle parton-medium interaction.”

High pT>60 GeV Z – Jet acoplanarity

ZHANG, LUO, WANG, AND ZHANG PHYSICAL REVIEW C **98**, 021901(R) (2018)

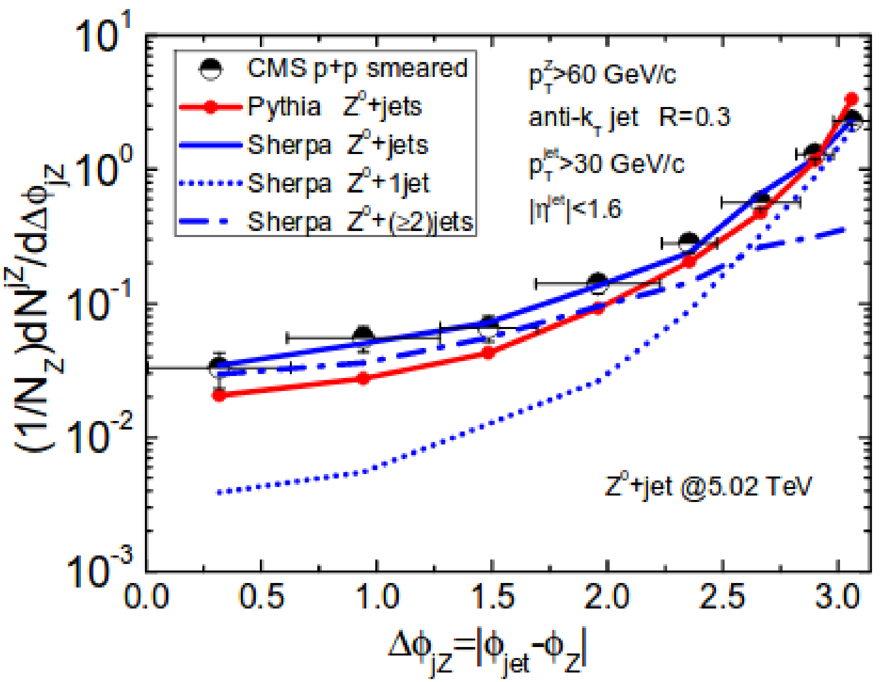

FIG. 1. Comparison between the azimuthal angle correlation $\Delta\phi_{jZ}$ of Z^0+jet by CMS data [28] and theoretical simulations of SHERPA (Blue) and Pythia (Red) in p+p collisions at $\sqrt{s} = 5.02$ TeV. The dotted (the dash-dotted) line shows the contribution from $Z^0 +$ 1jet ($Z^0 + (\geqslant 2)$jets).

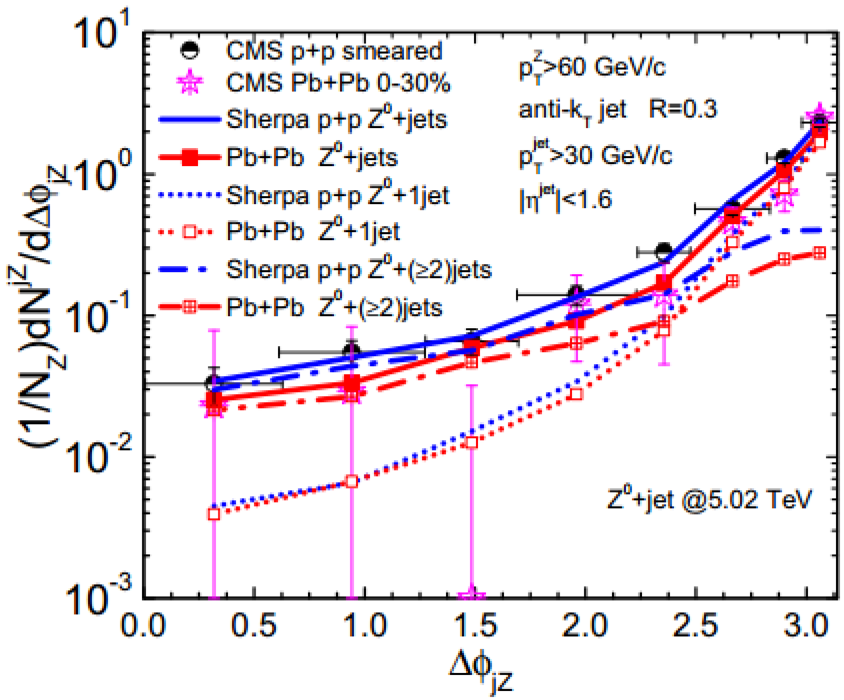

FIG. 5. Numerical results of the azimuthal angle correlation in $\Delta\phi_{jZ}$ in p+p (blue) and Pb+Pb (red) collisions at $\sqrt{s} = 5.02$ TeV as compared to CMS data [28]. The dotted (dash-dotted) lines show the contributions from Z^0 + 1jet ($Z^0 + (\geqslant 2)$jets).

decorrelation of the Z^0+jet in azimuthal angle from Z^0 + 1jet processes in this region is dominated by soft and collinear radiation, the resummation of which can be described by a Sudakov form factor. The transverse momentum broadening of this leading jet due to jet-medium interaction is negligible to that caused by soft and collinear radiation .

future experimental data with much better statistics are needed to observe this suppression of the small-angle Z^0+jet correlation unambiguously.

Section 2: Some details of the calculation

History of Acoplanarity : > 30 years ago !

D.Appel 1986

J.P.Blaizot, L.McLerran(1986); M. Greco,(1985); V. Sudakov (1956)

Acoplanarity in p+p is due to Gluon radiation from dijet antenna

In the parton model there are no bremsstrahlung effects, so we have simply $dP/dK_\eta=\delta(K_\eta)$. With perturbative QCD, multiple gluon emission from the hard scattering can be resummed in perturbation theory,[14] and for the one-dimensional normal momentum density has the form

$$\frac{1}{\sigma_0(p,p_T)}\frac{1}{p_T}\frac{d\sigma}{d\phi}=\frac{dP}{dK_\eta}=\frac{1}{\pi}\int_0^\infty db\cos(K_\eta b)\exp[\widetilde{B}(b)]\,.$$

In Double leading log Sudakov approx

$$\widetilde{B}(b)=-\int_{(b_0/b)^2}^{Q^2}\frac{dq^2}{q^2}\left[\ln\left[\frac{Q^2}{q^2}\right]A'(\alpha_s(q))+B'(\alpha_s(q))\right]$$

Acoplanarity in A+A arises from convolution of Sudakov and Jet-medium multiple scattering probabilities

$$F(\ell_T)\propto L\,\rho\,d\sigma/d^2\ell_T$$

Depends on the medium

$$\frac{dP}{dK_\eta}=\sum_{n=0}^{\infty}\sum_{m=0}^{\infty}\left[\frac{1}{n!}\prod_{i=1}^{n}\int d^2k_{Ti}B(\mathbf{k}_{Ti})\frac{1}{m!}\prod_{j=1}^{m}\int d^2l_{Tj}F(l_{Tj})\delta\left[K_\eta-\sum_{i=1}^{n}(\mathbf{k}_{Ti})_\eta-\sum_{j=1}^{m}(l_{Tj})_\eta\right]\right]$$

$$\int_{-\infty}^{+\infty}dK_\eta\exp(iK_\eta b)\frac{dP}{dK_\eta}=\exp[\widetilde{B}(b)+\widetilde{F}(b)]$$

D.Appel 1986

Jet Scattering in multi-component partonic plasmas

For $F(l_T)$, the probability density for scattering elastically off the plasma constituents with transverse-momentum transfer l_T, we propose the following form:

$$F(l_T)=\sum_x n_x R \frac{d^2\sigma_x}{d^2 l_T} \ , \qquad (11)$$

where x runs over the different particle types comprising the plasma $(x=g,q_i,\bar{q}_i)$, with n_x their number density. This equation essentially relates the plasma mean free path to the available distance for scattering (R) for each particular l_T.

$$F(l_T)=9aRT^3\left[1+\frac{N_F}{4}\right]\frac{\alpha_s^2(l_T)}{l_T^4}$$

Stefan-Boltzmann wQGP model estimates

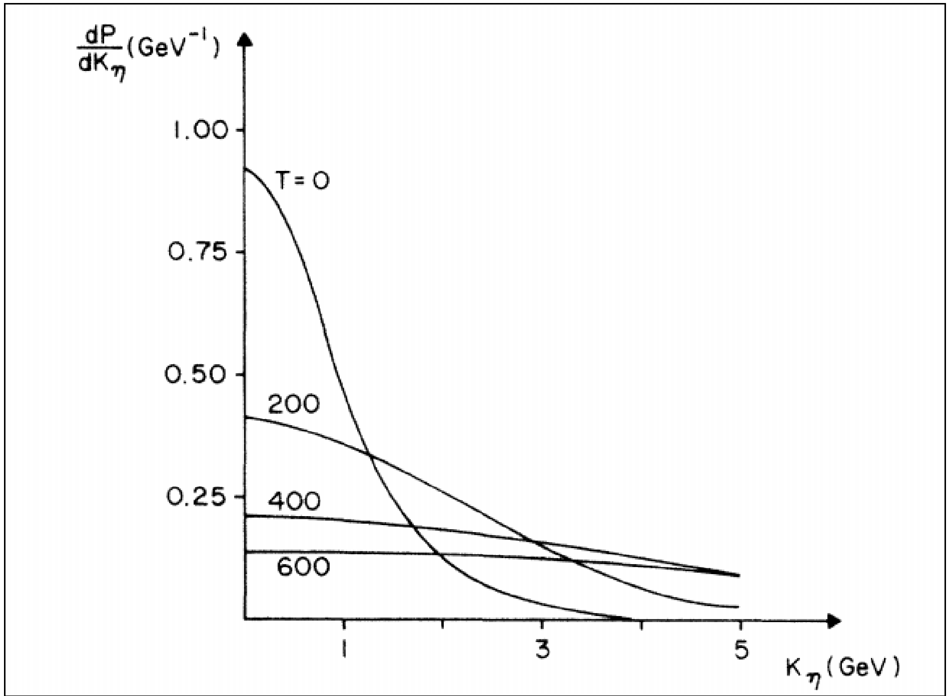

Cut off soft divergence below pQCD Debye mass

$$\ell_\perp \sim gT$$

"Based on this, one is encouraged to conjecture that someday jet behavior could be used as an effective thermometer of a QCD plasma."

Confirmed by J.P.Blaizot, L.McLerran(1986)
In more realistic detail

PHYSICAL REVIEW D VOLUME 24, NUMBER 5 1 SEPTEMBER 1981

Logarithmic approximations, quark form factors, and quantum chromodynamics

S. D. Ellis, N. Fleishon, and W. J. Stirling

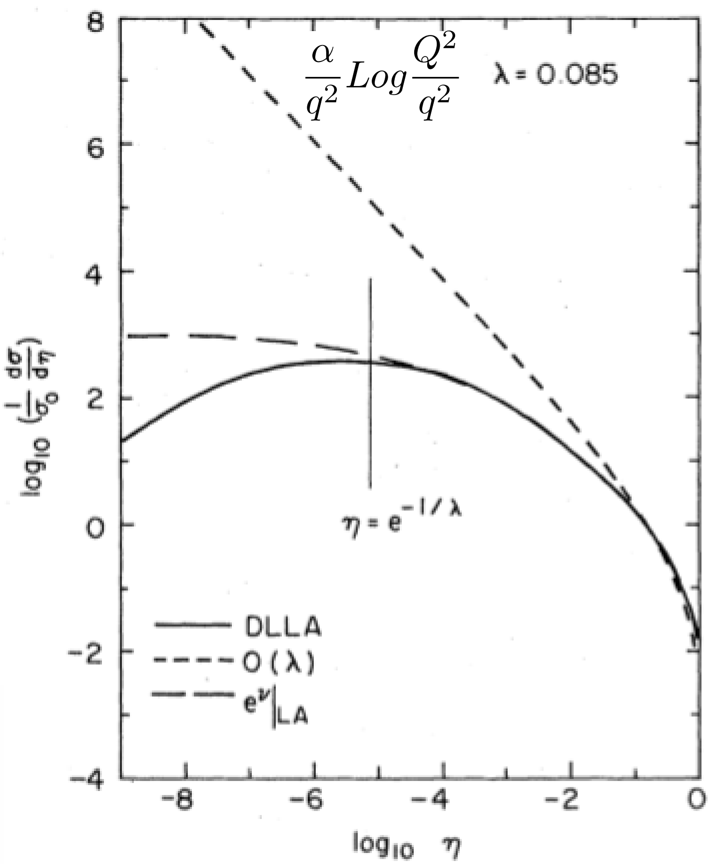

FIG. 4. Theoretical approximations to the cross section defined in the text. The long-dashed line is the soft logarithmic approximation [LA, (1), (2), (3)]. The solid line is the DLLA Eq. (2.12). The dashed line is the corresponding one-gluon contribution.

It is convenient to return to the general notation of the Introduction and define $\eta = Q_T{}^2/s$ and $\lambda = \alpha_s C_F/\pi$. Thus Eq. (2.11) can be written as

$$\frac{1}{\sigma_0}\frac{d\sigma}{d\eta}\bigg|_{\text{DLLA}} = \frac{\lambda}{\eta}\ln\frac{1}{\eta}\exp\left(-\frac{\lambda}{2}\ln^2\eta\right)\theta(1-\eta)$$
$$= \frac{d}{d\eta}F_{\text{DLLA}}(\eta)\theta(1-\eta) \qquad (2.12)$$

with $F_{\text{DLLA}}(\eta)$ identified from Eq. (1.1).

with $C_F = \frac{4}{3}$, $T_R = \frac{1}{2}$ and $N = 3$. It is instructive to see how the logarithms in b-space generate logarithms in q_T-space. For illustration, we take only the leading coefficient $A^{(1)} = 2C_F$ to be non-zero in $e^{S(b,Q^2)}$, and assume a fixed coupling α_S. This corresponds to

$$\frac{d\sigma}{dq_T^2} = \frac{\sigma_0}{2}\int_0^\infty b\, db\, J_0(q_T b)\exp\left[-\frac{\alpha_s C_F}{2\pi}\ln^2\left(\frac{Q^2 b^2}{b_0^2}\right)\right]. \qquad (6)$$

The expressions are made more compact by defining new variables $\eta = q_T^2/Q^2$, $z = b^2 Q^2$, $\lambda = \alpha_S C_F/\pi$, $z_0 = 4\exp(-2\gamma_E) = b_0^2$. Then

$$\frac{1}{\sigma_0}\frac{d\sigma}{d\eta} = \frac{1}{4}\int_0^\infty dz J_0(\sqrt{z\eta})\, e^{-\frac{\lambda}{2}\ln^2(z/z_0)} \qquad (7)$$

and we encounter the same expression as in [6], which describes the emission of soft and collinear gluons with transverse momentum conservation taken into account. The result

A. Kulesza, W.J. Stirling/Nuclear Physics B 555 (1999) 279–305

The conclusion is then that the *subleading logarithms* which arise from a correct treatment of transverse-momentum conservation can play a major role in filling in the zero at $\eta = 0$ and obscuring the maximum which was present near $\ln 1/\eta \sim 1/\lambda$ in the DLLA. It is informative to di-

$$\frac{dN_{BDMS}}{dq_T^2} = \frac{e^{-q_T^2/Q_s^2}}{Q_s^2} \quad \text{versus} \quad \frac{dN_{GLV}}{dq_T^2} = f(q_T, \mu, \chi)$$

GLV, PRD66, 014005 (2002)

Moliere Gaussian (Qs) vs Elastic scattering opacity series $(\mu, \chi = L/\lambda,\ Q_s^2 = \chi\mu^2\zeta)$

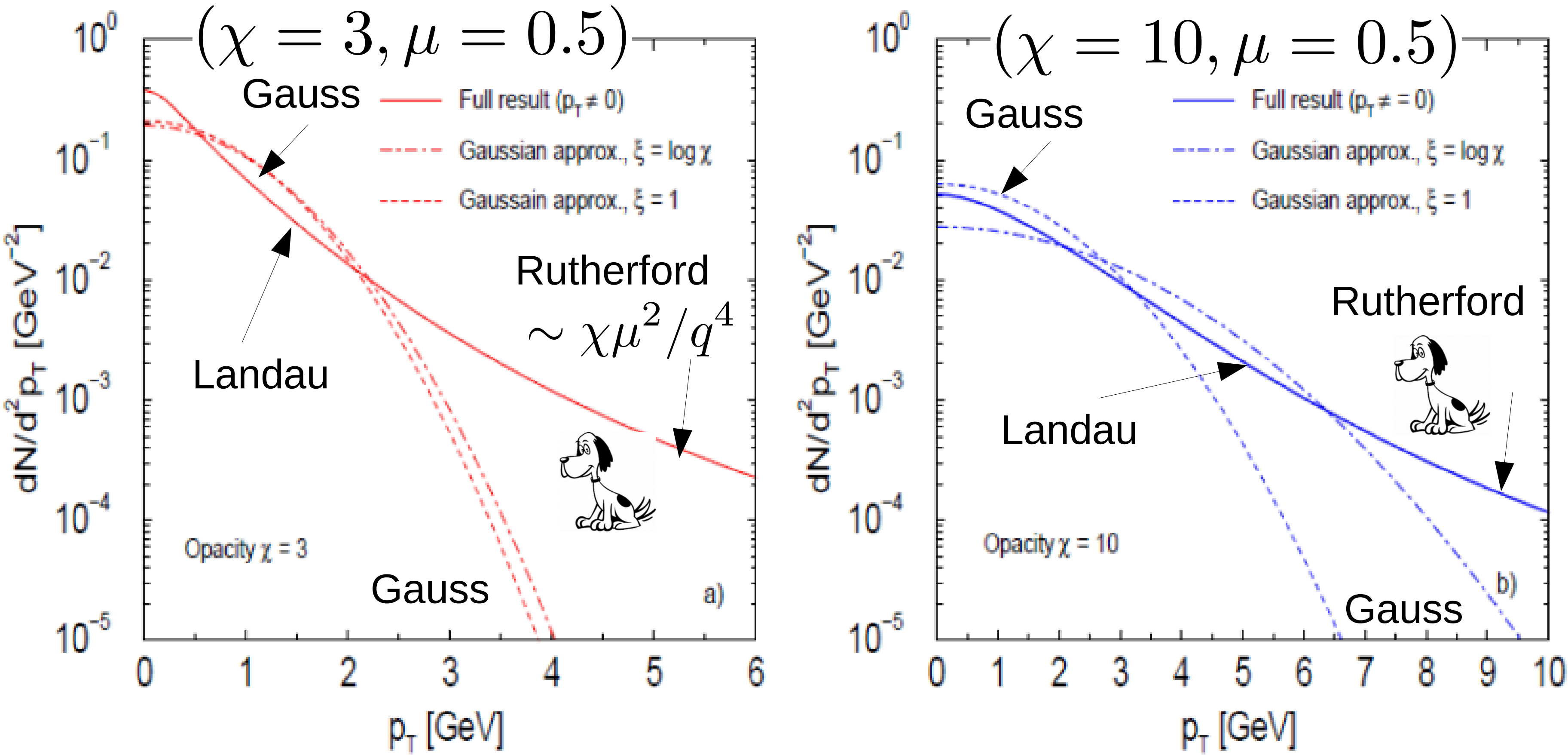

FIG 3. The final jet p_T distribution is shown versus p_T for two different opacities $\chi = 3$ (Fig. 3a) and $\chi = 10$ (Fig. 3b). We compare the full result (without the delta function contribution at $p_T \sim 0$) to the Moliere Gaussian approximation with $\xi = 1$ and $\xi = \log\chi$. In this example we use $\mu^2 = 0.25$ GeV^2.

Medium Induced Acoplanarity *Distribution* *shapes* due to multiple collisions depend on *at least* two parameters (μ, χ)

GLV PRD66 (2002)

e.g Yukawa μ≈ gT screened parton elastic scattering

$$\frac{d\tilde{\sigma}_{el}}{d^2\mathbf{q}}(\mathbf{b}) = \int \frac{d^2\mathbf{q}}{(2\pi)^2} e^{-i\mathbf{q}\cdot\mathbf{b}} \frac{1}{\pi} \frac{\mu^2}{(\mathbf{q}^2+\mu^2)^2} = \frac{\mu b}{4\pi^2} K_1(\mu b)$$

Mult.coll. opacity χ^n series can be summed in b-space

$$dN(\mathbf{p}) = e^{-\sigma_{el}T(\mathbf{b}_0)} \int d^2\mathbf{b} e^{i\mathbf{p}\cdot\mathbf{b}} e^{\tilde{\sigma}_{el}(\mathbf{b})T(\mathbf{b}_0)} dN^{(0)}(\mathbf{b})$$

$$\chi = \langle L/\lambda \rangle = \int \mathbf{dt} \int \mathbf{d^2q}\ \{\mathbf{d\sigma_{el}(t)/d^2q}\}\ \rho(\mathbf{t}, \mathbf{b_0}) \sim O(\alpha T L)$$

$$dN(\mathbf{p} \gg \chi\mu^2\xi) \approx (\chi\mu^2\xi)/\mathbf{p}^4$$

Rutherford tail

PHYSICAL REVIEW D **66**, 014005 (2002)

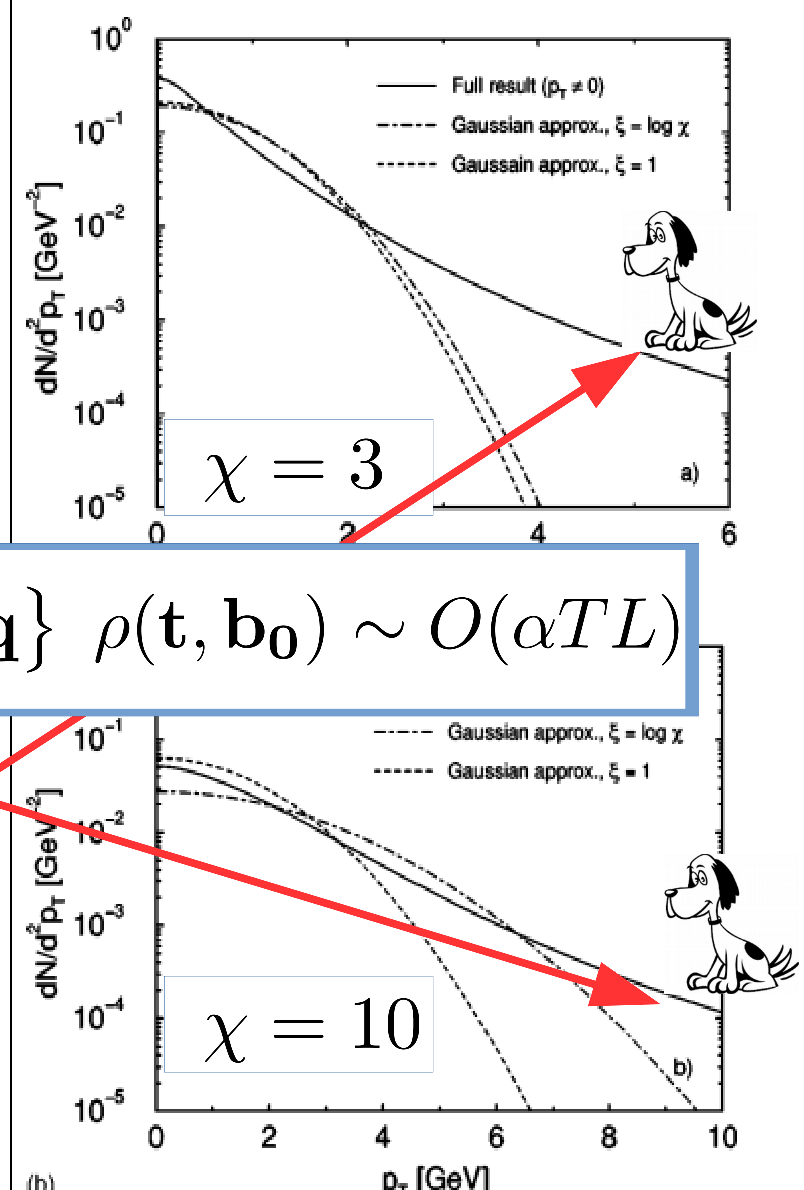

FIG. 3. The final parton p_T distribution is shown versus p_T for two different opacities $\chi=3$ (a) and $\chi=10$ (b). We compare the full result (without the delta function contribution at $p_T \sim 0$) to the Moliere Gaussian approximation with $\xi=1$ and $\xi=\log\chi$. In this example we use $\mu^2=0.25$ GeV^2.

In large χ>>1 lim, distrib. approaches Moliere form

$$dN(\mathbf{p}) = \int d^2\mathbf{b} e^{i\mathbf{p}\cdot\mathbf{b}} \frac{1}{(2\pi)^2} \frac{e^{-\chi\mu^2\xi b^2/2}}{\chi\mu^2\xi} = \frac{1}{2\pi} \frac{e^{-p^2/2\chi\mu^2\xi}}{\chi\mu^2\xi}$$

In BDMS approx this Gaussian form depends on only one "saturation scale"

$$Q_s^2 = \chi\mu^2\xi = \int dt\hat{q}(t)$$

Section 3: Numerical examples and conclusions

Summary of medium pT broadening distribution

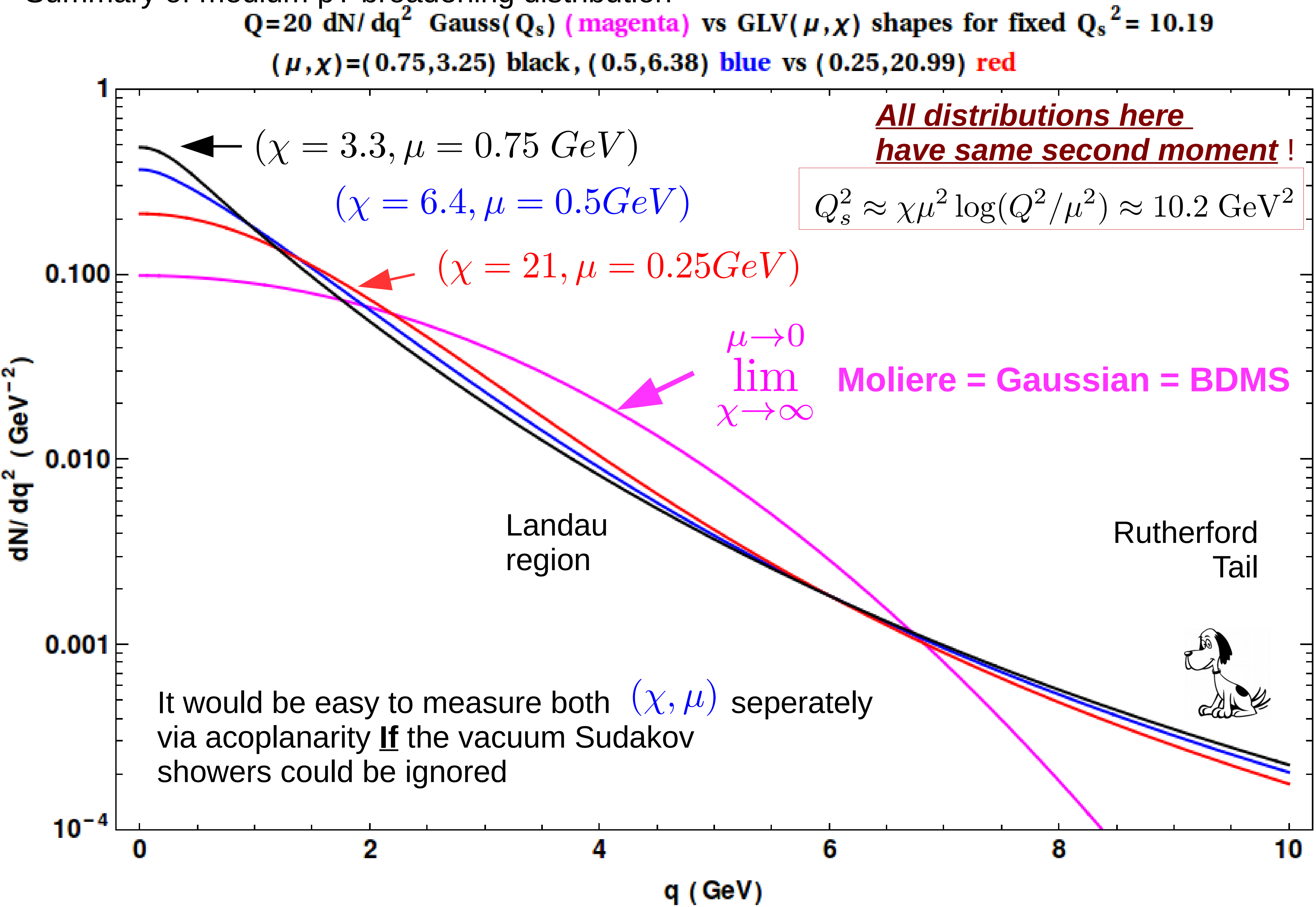

Summary 2:

Vacuum Sudakov dominates over medium induced dijet acoplanarity as Mueller et al and Chen et al emphasized

Percent level precision would be needed to resolve BDMS Qs into (χ, μ)

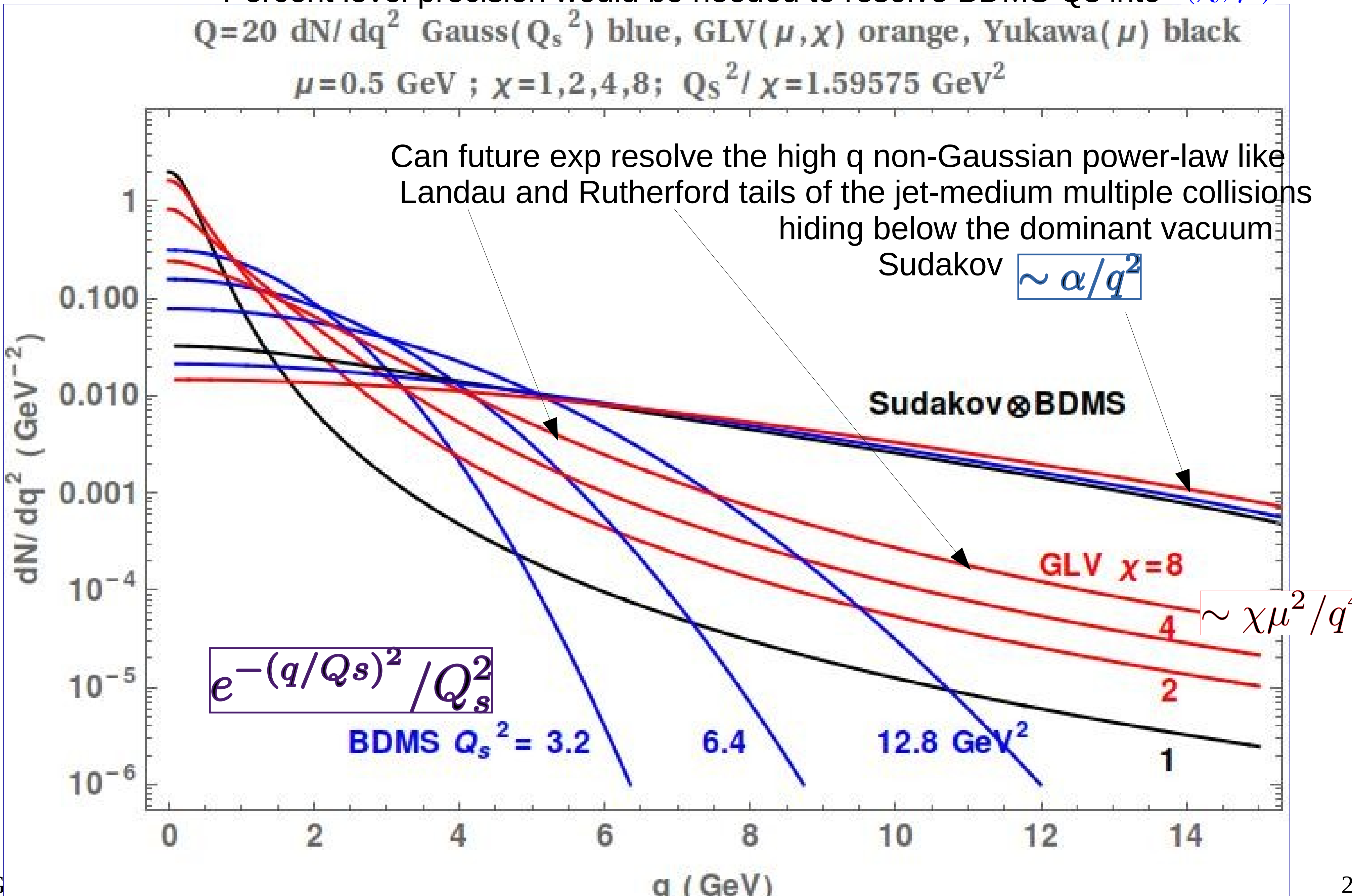

One parameter, Q_s, BDMS medium convoluted with Sudakov dijet transverse distributions

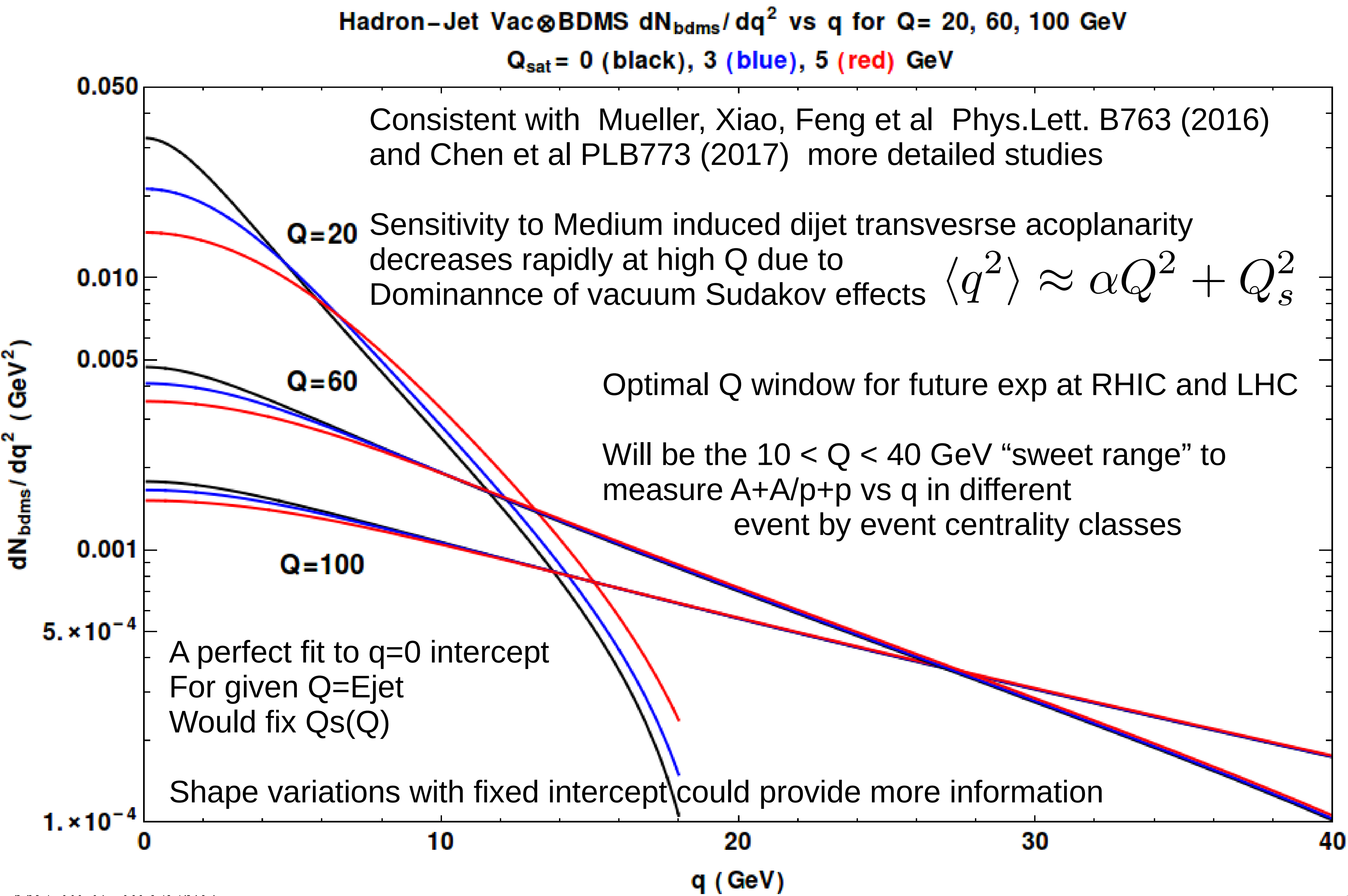

Consistent with Mueller, Xiao, Feng et al Phys.Lett. B763 (2016) and Chen et al PLB773 (2017) more detailed studies

Sensitivity to Medium induced dijet transvesrse acoplanarity decreases rapidly at high Q due to Dominannce of vacuum Sudakov effects $\langle q^2 \rangle \approx \alpha Q^2 + Q_s^2$

Optimal Q window for future exp at RHIC and LHC

Will be the 10 < Q < 40 GeV “sweet range” to measure A+A/p+p vs q in different event by event centrality classes

A perfect fit to q=0 intercept
For given Q=Ejet
Would fix Qs(Q)

Shape variations with fixed intercept could provide more information

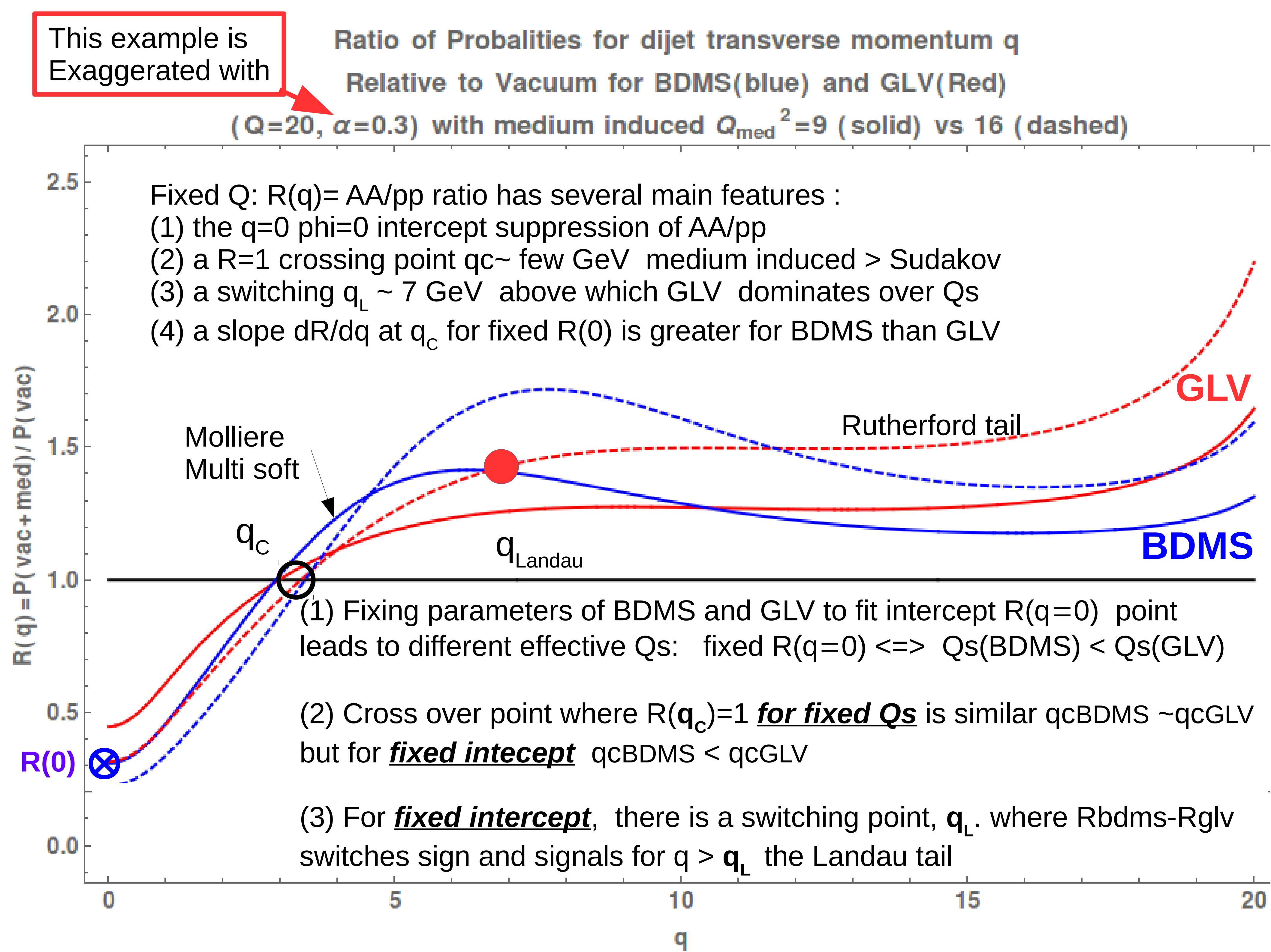
This example is Exaggerated with
Ratio of Probalities for dijet transverse momentum q
Relative to Vacuum for BDMS(blue) and GLV(Red)
(Q=20, α=0.3) with medium induced Q_{med}^2=9 (solid) vs 16 (dashed)
Fixed Q: R(q)= AA/pp ratio has several main features :
(1) the q=0 phi=0 intercept suppression of AA/pp
(2) a R=1 crossing point qc~ few GeV medium induced > Sudakov
(3) a switching q_L ~ 7 GeV above which GLV dominates over Qs
(4) a slope dR/dq at q_C for fixed R(0) is greater for BDMS than GLV
GLV
Rutherford tail
Molliere
Multi soft
q_C
q_{Landau}
BDMS
(1) Fixing parameters of BDMS and GLV to fit intercept R(q=0) point
leads to different effective Qs: fixed R(q=0) <=> Qs(BDMS) < Qs(GLV)
(2) Cross over point where R(q_C)=1 for fixed Qs is similar qcBDMS ~qcGLV
but for fixed intecept qcBDMS < qcGLV
(3) For fixed intercept, there is a switching point, q_L. where Rbdms-Rglv
switches sign and signals for q > q_L the Landau tail
R(0)
R(q)=P(vac+med)/P(vac)
q
0
5
10
15
20
0.0
0.5
1.0
1.5
2.0
2.5

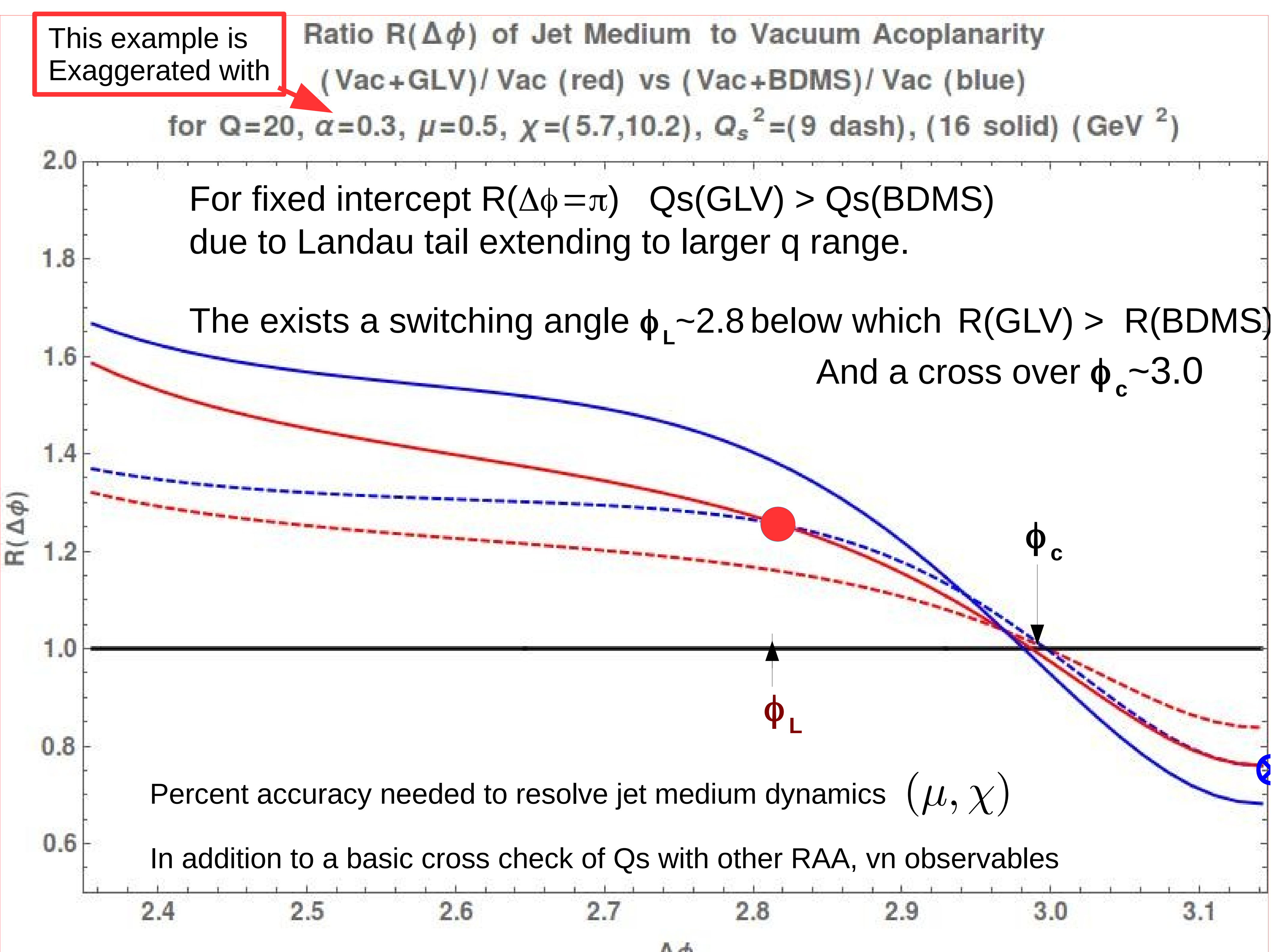
This example is Exaggerated with
Ratio R(Δϕ) of Jet Medium to Vacuum Acoplanarity
(Vac+GLV)/ Vac (red) vs (Vac+BDMS)/ Vac (blue)
for Q=20, α=0.3, μ=0.5, χ=(5.7,10.2), Qs²=(9 dash), (16 solid) (GeV ²)
For fixed intercept R(Δφ=π) Qs(GLV) > Qs(BDMS)
due to Landau tail extending to larger q range.
The exists a switching angle φL~2.8 below which R(GLV) > R(BDMS)
And a cross over φc~3.0
φc
φL
Percent accuracy needed to resolve jet medium dynamics (μ, χ)
In addition to a basic cross check of Qs with other RAA, vn observables
R(Δϕ)
Δϕ
2.0
1.8
1.6
1.4
1.2
1.0
0.8
0.6
2.4
2.5
2.6
2.7
2.8
2.9
3.0
3.1

For more realistic Sudakov fits to p+p set $\alpha \approx 0.09$
Requires much higher precision to resolve GLV finite (χ,μ) from BDMS(Qs)

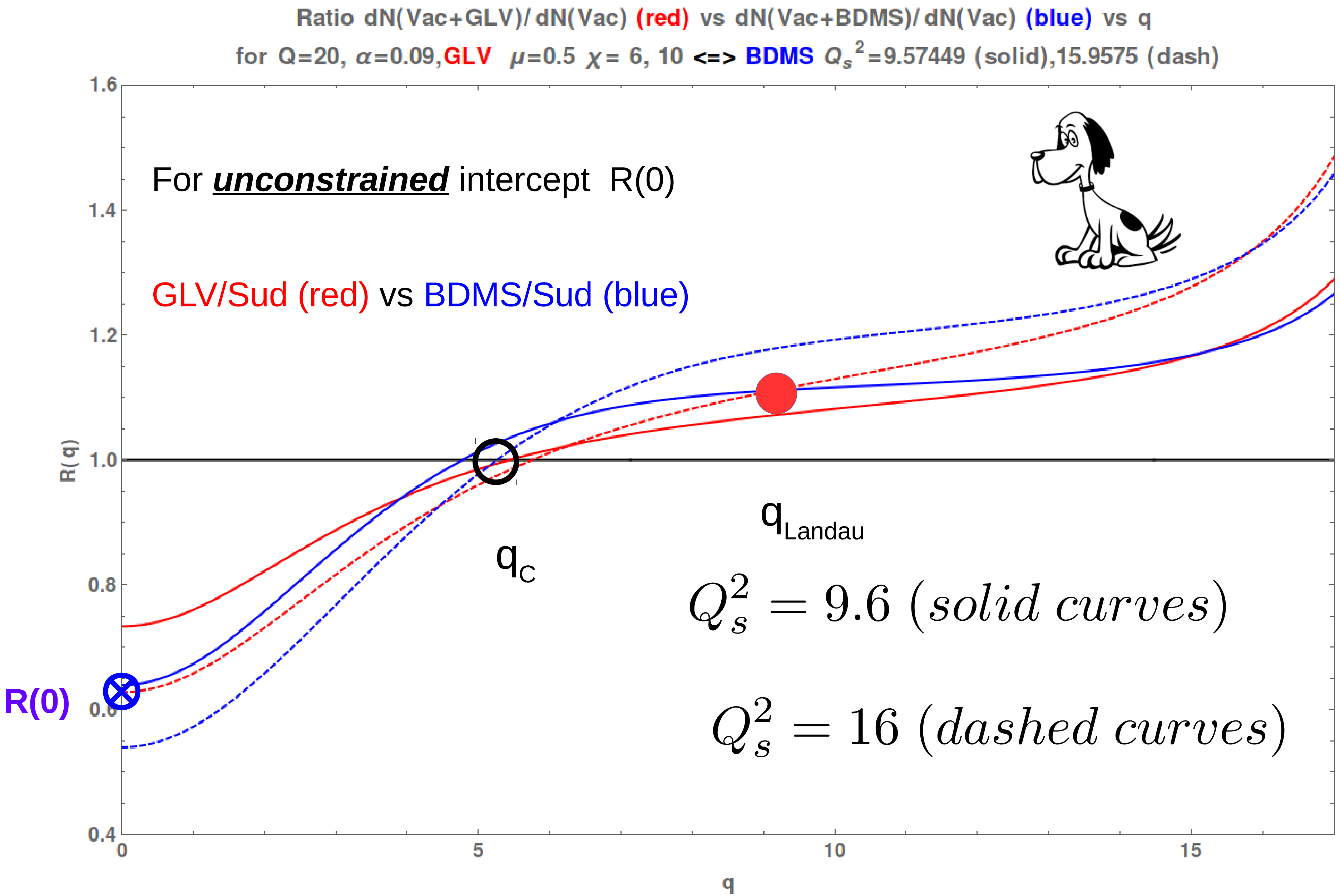

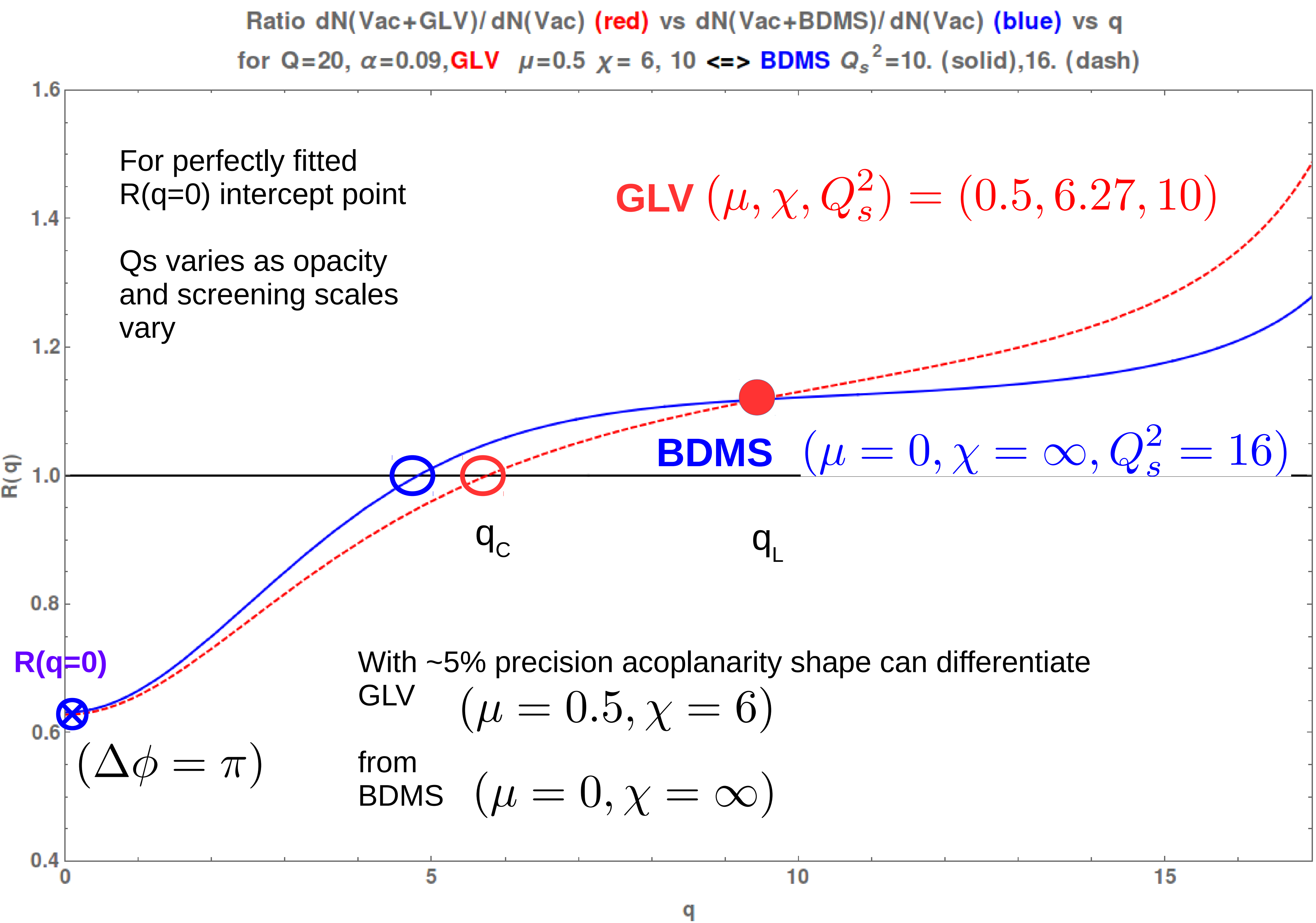

Ratio dN(Vac+GLV)/dN(Vac) (red) vs dN(Vac+BDMS)/dN(Vac) (blue) vs q
for Q=20, α=0.09, GLV μ=0.5 χ= 6, 10 <=> BDMS $Q_s{}^2$=10. (solid),16. (dash)
For perfectly fitted
R(q=0) intercept point
Qs varies as opacity
and screening scales
vary
GLV $(\mu, \chi, Q_s^2) = (0.5, 6.27, 10)$
BDMS $(\mu = 0, \chi = \infty, Q_s^2 = 16)$
q_C
q_L
R(q=0)
$(\Delta\phi = \pi)$
With ~5% precision acoplanarity shape can differentiate
GLV $(\mu = 0.5, \chi = 6)$
from
BDMS $(\mu = 0, \chi = \infty)$
R(q)
q
1.6
1.4
1.2
1.0
0.8
0.6
0.4
0
5
10
15

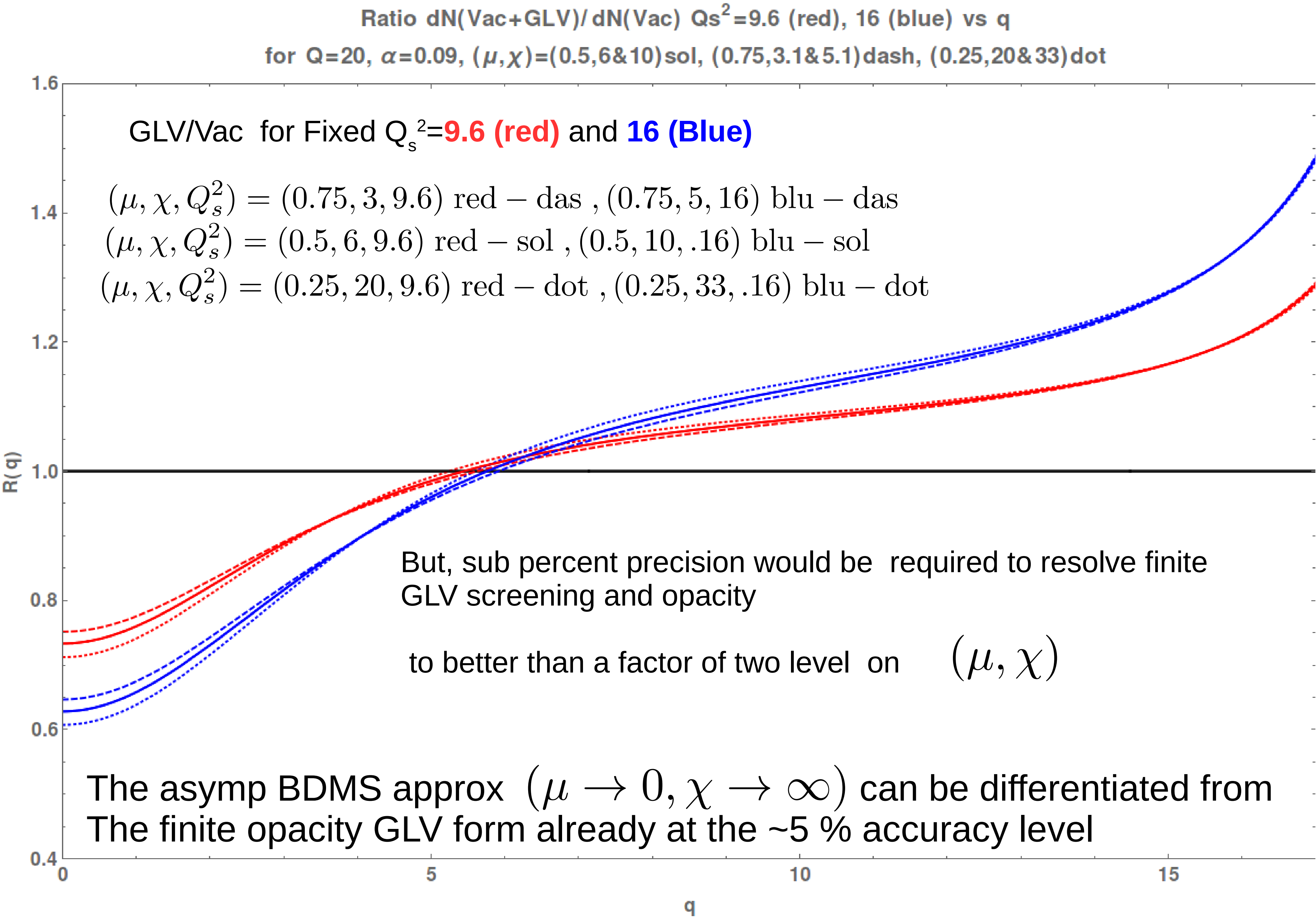
Ratio dN(Vac+GLV)/ dN(Vac) Qs^2=9.6 (red), 16 (blue) vs q
for Q=20, α=0.09, (μ,χ)=(0.5,6&10)sol, (0.75,3.1&5.1)dash, (0.25,20&33)dot
GLV/Vac for Fixed Q_s^2=9.6 (red) and 16 (Blue)
$(\mu,\chi,Q_s^2)=(0.75,3,9.6)$ red – das , $(0.75,5,16)$ blu – das
$(\mu,\chi,Q_s^2)=(0.5,6,9.6)$ red – sol , $(0.5,10,.16)$ blu – sol
$(\mu,\chi,Q_s^2)=(0.25,20,9.6)$ red – dot , $(0.25,33,.16)$ blu – dot
But, sub percent precision would be required to resolve finite GLV screening and opacity
to better than a factor of two level on (μ,χ)
The asymp BDMS approx $(\mu\to 0,\chi\to\infty)$ can be differentiated from The finite opacity GLV form already at the ~5 % accuracy level
R(q)
q
1.6
1.4
1.2
1.0
0.8
0.6
0.4
0
5
10
15

Final remarks:

Is the extra experimental and theoretical effort needed to try to extract dynamical information such as $\Gamma_{ab}(q_\perp, T) = \rho_b(T) d^2\sigma_{ab}(T)/d^2 q_\perp$ from the *very tiny* medium modifications of azimuthal acoplanarity observables worth it?

Yes, because we need more ways to falsify competing microscopic dynamical mechanisms such as critical opalescence in sQGMP or non-conformal holography to gain more insight into the novel chromo dynamics responsible for the observed perfect fluidity of the bulk in A+A and the intricate hard jet and dijet quenching patterns correlated So strongly with the soft perfect fluid flow observable

Appendix: extra slides and links to longer lectures

http://www.columbia.edu/~mg150/Talks/2017/MGyulassy-Lec1-CCNU-101817.pdf

http://www.columbia.edu/~mg150/Talks/2017/MGyulassy-Lec2-CCNU-101817.pdf

Conclusion 1:

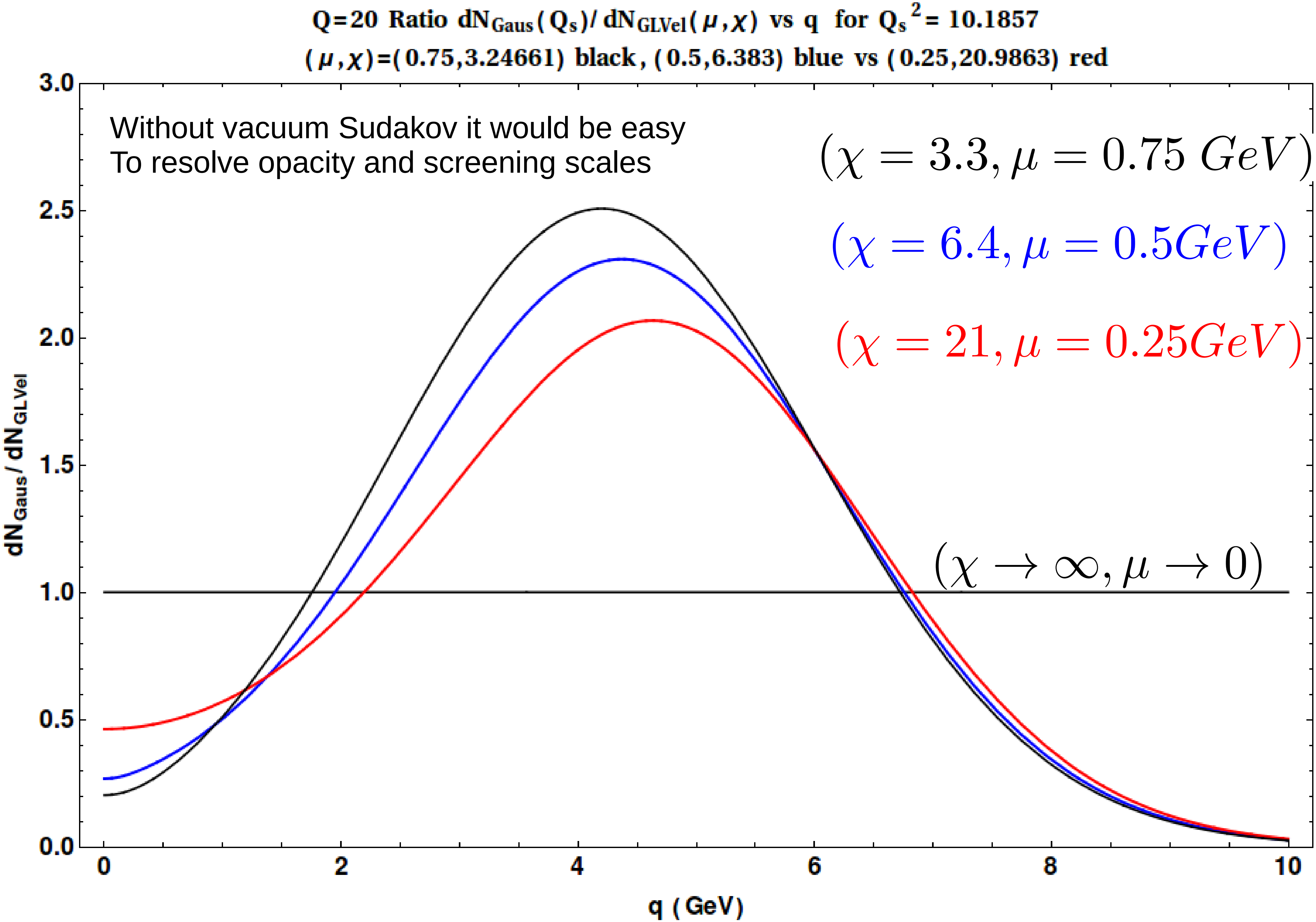

Angular structure of jet quenching within a hybrid strong/weak coupling model

Jorge Casalderrey-Solana et al JHEP03 (2017) 135

Hybrid: Pythia+ N=4 SYM holography model with added Gaussian transverse momentum
Distributed with BDMS Gaussian approximation controlled by a parameter K

$$Q_s^2 \equiv \langle \hat{q} L \rangle \equiv K \, \langle T^3 L \rangle$$

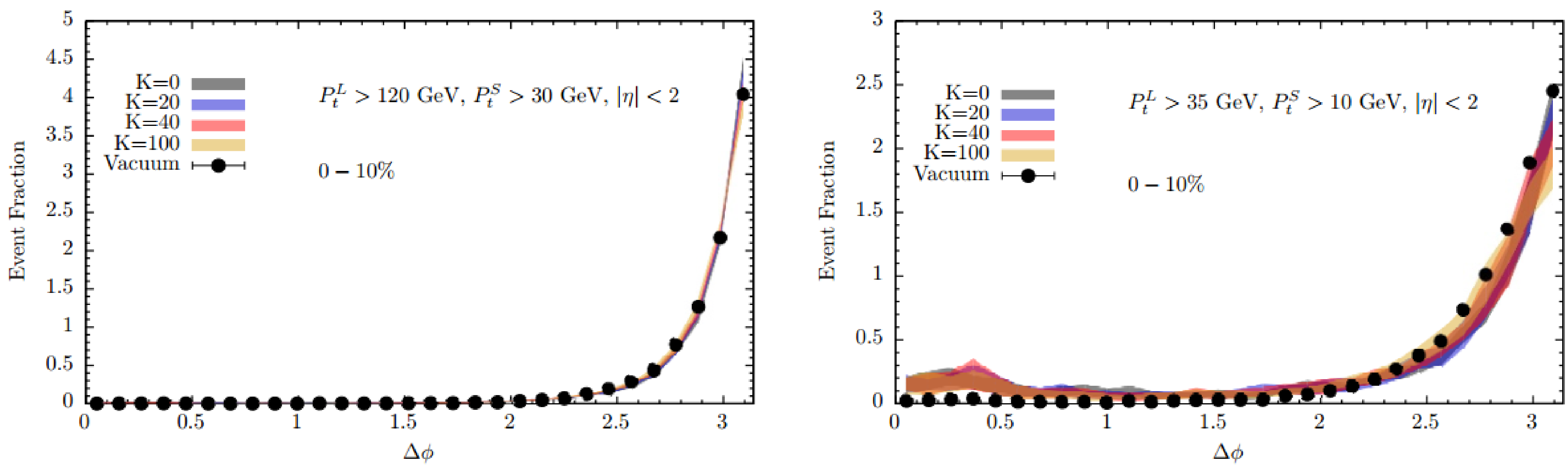

Figure 3. Dijet acoplanarity distribution for high-energy (left) and low-energy (right) dijets in LHC heavy ion collisions with $\sqrt{s} = 2.76$ ATeV for two different values of the broadening parameter K. For comparison, the black dots show the acoplanarity in proton-proton collisions as simulated by PYTHIA.

the effects of medium broadening on the acoplanarity distribution are small

For E ~ 30 GeV strong coupling broadenning could be tested in the future to falsify holographic or perturbative or other hybrid model combinations